NOVA SCHOOL OF SCIENCE & TECHNOLOGY

DEPARTMENT OF PHYSICS

ANDRÉ VIEIRA TRIGO DOS SANTOS COUTINHO

Bachelor of Science in Biomedical Engineering

MACROMOLECULAR CROWDING: ENHANCING CELL METABOLISM, ENHANCING REGENERATION

MASTER IN BIOMEDICAL ENGINEERING

NOVA University Lisbon
March, 2022

NOVA SCHOOL OF
SCIENCE & TECHNOLOGY

DEPARTMENT
OF PHYSICS

MACROMOLECULAR CROWDING: ENHANCING CELL METABOLISM, ENHANCING REGENERATION

ANDRÉ VIEIRA TRIGO DOS SANTOS COUTINHO

Bachelor of Science in Biomedical Engineering

Adviser: Jorge Carvalho Silva
Associate Professor, NOVA University Lisbon

Co-adviser: Tânia Vieira
Junior Researcher, NOVA University Lisbon

MASTER IN BIOMEDICAL ENGINEERING

NOVA University Lisbon
March, 2022

Macromolecular Crowding: Enhancing Cell Metabolism, Enhancing Regeneration

To my grandfather, Zacarias.

Acknowledgements

This dissertation marks the end of an important chapter in my life in which many people were involved. Although the final product of an almost 20 year educational journey may be a degree, that would be irrelevant without the people present along the way, which also take credit for my success.

Firstly, I'd like to thank all my professors, from elementary school to university. I believe that a good professor has the power to change the world of multiple children and students, and I was honoured to have a lot of them throughout my life. Thank you Professor Amélia, my elementary school teacher, Professor Cristina, my class director in middle school, and Professor António, my high school math teacher. I'd also like to show gratitude to my tutor, D. Ana, for all the years of extra hours to understand the (not-so) impossible.

Secondly, I'd like to thank my advisor, Professor Jorge Silva, for accepting me in this project and for all the orientation provided. Your knowledge and skill were important for the development of this work.

To my co-advisor, Doctor Tânia Vieira, I couldn't be more grateful to have shared the last months with you. Your know-how, constant orientation and availability, sense of humor, and friendship were extremely important for me. I'm sure I leave a better professional and human-being thanks to you.

I'd also like to thank Professor João Lourenço and collaborators for creating such an accessible template (NOVAThesis) which saved me an immense amount of time [1].

To my laboratory colleagues, I'd like to leave a word of appreciation for all the fun moments and all the advices. My daily basis in the laboratory was better because of you.

To all my friends, each and everyone of you played a part in molding the person I am today. You are extremely important in my life and I can only be grateful for everything. Firstly, I'd like to thank all my university friends for being present in my life along these 6 years, especially Melo, Silva, Mara, Maria, Catarina, Joana, Barrocas, Rosa and Feliz. Thank you for all the good moments, the bad moments, the get-togethers, the parties, the advice and the support. A special word for Melo, my partner in crime during these 6 years in university. You helped me in so many ways, and I'm glad I have you as my friend.

A word of appreciation to all the Ohana members and all the amazing people I came in touch with in this course and FCT.

Secondly, to my high school friends and the boys, it is always a pleasure to share a moment with you. Alberto, Botas, Cabral, Ismael, Johny, Pedro, Ramalho, Rodrigo, Tiago and Torres, thank you for all the jokery, the drinks, the dinners, the stupidity and the friendship.

A kind word to all the friends who I lost along this long path. You also contributed to the person I am today.

Lastly, to Ramalho, my brother from another mother, thanks for all the support and friendship. You are the most balanced and astute person I know, and your wisdom has helped me through the worst moments of my life.

These acknowledgements could not be completed without mentioning my family. Olinda, my mother, your nature and your love for me taught me invaluable things which I use in my life everyday and that make me a better man. Carlos, my father, I couldn't have asked for a better provider, and I deeply appreciate all the support you have given me throughout my life. Teresa, my grandmother, you are the most hard-working woman in the world. I cannot put in words the importance you have in my life. Thank you for everything. Zacarias, my grandfather, you were the toughest, yet kindest man I ever knew, and I hope I make you proud everyday. This one is for you. Rafa, my cousin, you are the brother I never had, and because of you I try to be the best big brother I could possibly be. I couldn't be more proud of you, and of the relationship we have. Carlos and Emília, my grandparents, thank you for all your unconditional support and love throughout my life. I wish I could spend more time with you. Cristina, Sofia, Zé, Tó and Pingurço, my aunts, borrowed-uncles and granduncle, I appreciate everything you have done for me, the availability and the support. A big thanks to each and everyone of the elements of my family, I love you all so much.

Abstract

Deep and extensive skin injuries represent a major worldwide healthcare problem without an efficient treatment option, with autologous skin grafts constituting the treatment gold standard. Tissue engineered skin constructs emerge as alternatives to this method, however, "cost-to-heal" factor or the need for long culture times are important drawbacks. The iSkin2 project aims to overcome these limitations, namely by incorporating the macromolecular crowding (MMC) effect, which shows potential in significantly reducing the prolonged healing times. This effect consists in emulating *in vitro* the heavily macromolecular-crowded *in vivo* environment, allowing to increase the rate of several biological reactions, namely cellular proliferation and extracellular matrix production.

This dissertation assessed if the MMC effect is beneficial for the increase of collagen type I and fibronectin deposition by dermal fibroblasts seeded on polycaprolactone (PCL) scaffolds, and, if it is, which studied crowding agent (Ficoll cocktail or polyvinylpyrrolidone 55 kDa) had the best results. For this, fibroblast viability was assessed in the matrices produced in the presence of the crowders, and immunocytochemistry procedures were performed to visualize and quantify the deposition of collagen type I and fibronectin in the constructs studied.

We showed that the use of Ficoll cocktail, although not reaching as good results as the ones in literature, outperformed the use of polyvinylpyrrolidone 55 kDa, offering an interesting alternative to the uncrowded cell medium. We also present evidences that show the potential of using the MMC effect in 3D environments, specifically in PCL matrices.

Keywords: Tissue Engineering, macromolecular crowding, polyvinylpyrrolidone, Ficoll, extracellular matrix, fibroblast, fibronectin, collagen, polycaprolactone, chitosan, gelatin

Resumo

Lesões extensas e profundas na pele representam um problema de saúde significativo a nível mundial sem uma opção de tratamento eficiente, sendo os enxertos de pele autólogos o tratamento *gold standard*. A engenharia de tecidos surge como alternativa a estes métodos através da criação de substitutos de pele. No entanto, a relação custo-benefício ou a necessidade de longos tempos de cultura constituem desvantagens importantes. O projeto iSkin2 pretende ultrapassar estas limitações, nomeadamente incorporando o efeito *macromolecular crowding* (MMC), que demonstra potencial em reduzir significativamente os tempos de tratamento. Este efeito consiste em simular *in vitro* o ambiente extremamente abundante em macromoléculas verificado *in vivo*, permitindo o aumento da taxa de várias reações biológicas, nomeadamente a proliferação celular e a produção de matriz extracelular.

Esta dissertação explorou se o efeito MMC contribui para o aumento da deposição de colagénio tipo I e fibronectina por parte de fibroblastos semeados em matrizes de policaprolactona (PCL), e qual a macromolécula (cocktail Ficoll ou polivinilpirrolidona 55 kDa) com os melhores resultados. Para isto, foram realizados estudos de viabilidade em fibroblastos semeados nas matrizes de PCL na presença das macromoléculas, e procedimentos de imunocitoquímica para visualizar e quantificar a deposição de colagénio tipo I e fibronectina.

Aqui demonstrou-se que o uso de cocktail Ficoll, apesar de não atingir resultados tão bons como os existentes na literatura, superou o uso de polivinilpirrolidona 55 kDa, oferecendo uma alternativa interessante à utilização de meio de cultura sem macromoléculas. Também ficaram demonstradas evidências que indicam o potencial do uso do efeito MMC em ambientes 3D, especificamente em matrizes de PCL.

Palavras-chave: Engenharia de tecidos, *crowding* macromolecular, polivinilpirrolidona, Ficoll, matriz extracelular, fibroblasto, fibronectina, colagénio, policaprolactona, quitosano, gelatina

Contents

List of Figures

List of Tables

Glossary

4',6-Diamidino-2-phenylindole	Fluorescence stain that binds to adenine-thymine-rich regions in cell DNA
Allogenic	Taken from different individuals of the same species
Angiogenesis	Physiological process through which new blood vessels are formed
Autocrine	Form of signalling in which a cell secretes a hormone or a chemical agent that acts in the same cell
Autologous	Derived from the same individual
Carrageenan	Negatively charged natural polysaccharide obtained by extraction of red seaweeds
Chondrocyte	Cells found in cartilagenous tissue
Collagen	Main structural protein in the extracellular matrix of connective tissues. There are various type of collagens, namely collagen type I, III, VI and VII
Connective tissue	One of the four basic types of tissue in animals. Found in regions in between the other tissues.
Crosslinking	Bond that links one polymer chain to another
Dextran sulfate	Synthetic sulfated polysaccharide derived from the condensation of glucose
Differentiation	Process in which a cell alters from one phenotype to another
Epithelial tissue	One of the four basic types of tissue in animals. Forms the covering of all body surfaces, body cavities and hollow organs

Excluded volume effect	Effective volume that is inaccessible to other molecules in a solution due to the presence of the first molecule
Extracellular Matrix	Non-cellular component present within all tisues and organs, containing an array of multidomain macromolecules which provide phyiscal, biochemical and biomechanical support to the cells
Fibroblast	Most common cell type found in connective tissues and dermis
Fibronectin	Glycoprotein present in the extracellular matrix. Plays a major role in cell adhesion, growth, migration and differentiation
Ficoll	Neutral, hydrophilic polysaccharide. Has several applications in biological laboratories
Fractional volume occupancy	Fraction of the total volume occupied by macromolecules
Glycosaminoglycan	Negatively charged polysaccharide compounds found in the extracellular matrix of mammalian cells
Growth factor	Diffusible signaling proteins that stimulate cell growth, inflammation, differentiation, survival, etc
Hyaluronic acid	Non-sulfated glycosaminoglycan present in connective, epithelial and neural tissues
Hydrodynamic radius	Radius of a hard sphere that diffuses at the same rate as that solute
Keratinocyte	Most common cell type found in epidermis
L-ascorbic acid 2-phosphate	Better known as vitamin C. Has antioxidant properties and promotes collagen formation in various tissues
Matrix metalloproteinase	Enzymes capable of breaking down proteins, playing a major role in wound healing
Mesenchymal stem cells	Multipotent cells that can differentiate into a variety of cell types
Mowiol	Hydrophilic mounting medium for immunofluorescence and molecular biology applications

Oxygen tension	Partial pressure of the dissolved oxygen within a tissue
Podocyte	Highly specialized epithelial cells that cover the outside of the glomerular capillary, in the kidneys
Polydispersity	Indicates the breadth or width of the molecular weight distribution. Describes the degree of non-uniformity of the distribution.
Polyvinylpyrrolidone	synthetic polymer with several biomedical applications
Procollagen	Percursor of collagen
Proteoglycan	Glycosaminoglycans covalently attached to core proteins
Scaffold	Engineered materials to provide support for the growth of cells into functional tissues
Steric hindrance	Congestion caused by repulsive forces between overlapped electron clouds
Tenocyte	Tendon cell

Acronyms & Abbreviations

AA	l-ascorbic acid 2-phosphate
bFGF	fibroblast growth factor
BSA	bovine serum albumin
CR	carrageenan
CS	chitosan
DAPI	4',6-diamidino-2-phenylindole
DEJ	dermal-epidermal junction
DHT	dehydrothermal
DMEM	Dulbecco's modified Eagle's medium
Dx	Dextran
DxS	Dextran sulfate
ECM	extracellular matrix
EDC/NHS	N-ethyl-N'-(3-(dimethylamino)propyl)carbodiimide/N-hydroxysuccinimide
EVE	excluded volume effect
FBS	foetal bovine serum
Fc	Ficoll
FVO	fractional volume occupancy
GAG	glycosaminoglycan
GDF5	growth differentiation factor 5
GEL	gelatin
GTA	glutaraldehyde

HA	hyaluronic acid
HFFF2	human caucasian foetal foreskin fibroblasts
IGF-1	insulin-like growth factor 1
IL1	interleukin 1
KGF	keratinocyte growth factor
MGV	mean gray value
MMC	macromolecular crowding
MSC	mesenchymal stem cell
MW	molecular weight
OD	optical density
PBS	phosphate buffered saline
PCL	polycaprolactone
PDGF	platelet-derived growth factor
Pen Strep	penicillin/streptomycin
PEO	poly(ethylene oxide)
PFA	paraformaldehyde
PLLA	poly(l-lactic acid)
PSS	polysodium-4-styrene sulfonate
PVP	polyvinylpyrrolidone
RCF	relative centrifugal force
RM	regenerative medicine
RT	room temperature
RT-qPCR	real-time quantitative polymerase chain reaction
TE	tissue engineering
TERM	tissue engineering and regenerative medicine
TGF	transforming growth factor
VEGF-A	vascular endothelial growth factor A

1

Introduction

This chapter starts by explaining the context and the motivation behind this dissertation. The second section identifies the goal to be achieved with this work and the various objectives to be accomplished to reach that goal. Lastly, the third section provides the thesis outline.

1.1 Context and Motivation

Deep and extensive skin wounds represent a major worldwide healthcare problem resulting from a significant prevalence of physical trauma or wound-healing-affecting pathologies. The gold standard to treat such injuries is the use of autologous skin grafts. However, in patients with extensive skin loss, such strategy is not viable. Allogenic skin graft is another alternative to treat these wounds, but limited availability and immunological rejection remain major challenges. Tissue engineering and regenerative medicine (TERM) techniques emerge as alternatives to the referred conventional transplantation procedures, with some bioengineered scaffolds and wound dressings already possessing clinical relevance for the treatment of such injuries. However, there is still a long path ahead before tissue engineered skin substitutes become a real alternative to the gold standard procedures, as anatomical, physiological and aesthetic limitations are still accentuated. Additionally, 'cost-to-heal' factor remains a huge bottleneck for an extended clinical application of such therapies. Thus, there is a need for further investigation in TERM for the development of improved and more efficient engineered skin substitutes.

Considering this, the iSkin2 project, in which this dissertation is inserted, aims to overcome such limitations and develop a cost-efficient skin substitute for the treatment of patients with extensive skin loss, such as the ones resulting from second- and third-degree burns. This dermal-epidermal substitute, Skin2, is expected to provide a cutting edge, low-cost solution available to be applied to the patient within hours of being admitted to the hospital, offering a complete therapeutic alternative, while only relying on biodegradable materials and cells extracted from the patient. Several activities were performed or are underway in the context of this project. Good results regarding the

assembly of the dermal scaffold, a matrix produced by the electrospinning of chitosan (CS), gelatin (GEL) and polycaprolactone (PCL), were achieved.

This dissertation aims to understand the effect of macromolecular crowding (MMC) in the regenerative and metabolic activity of skin cells, specifically fibroblasts, seeded on the referred dermal scaffold. Briefly, the MMC concept defends that emulating a highly crowded environment *in vitro* such as the one present *in vivo* (in physiological tissue, the media is abundant in molecules) enhances the rate of several biological processes, such as extracellular matrix (ECM) production and deposition. Therefore, by applying this concept in the assembly of skin substitutes, it is expected that their high production time, which is directly influenced by the elevated cell culture time, is significantly reduced. Considering that the current skin substitutes using autologous cells need 2 to 3 weeks of culture time before use, and that patients usually require immediate treatment, this readiness provided by MMC could have immense impact in the clinical context.

Several cultures of fibroblasts in the various materials composing of the dermal scaffold were performed. To assess the influence of MMC in the activity of fibroblasts in the referred materials, two different crowders were used: Ficoll 70 kDa and Ficoll 400 kDa mixture, and polyvinylpyrrolidone (PVP) 55 kDa. Two different techniques were used to study the effect of these crowders: immunocytochemistry, to study the effect of MMC in ECM deposition, and resazurin assays, to assess how MMC influences fibroblast viability.

1.2 Objectives

The main goal of this dissertation is to determine if the implementation of the MMC effect in the dermal scaffold seeded with fibroblasts is beneficial for the increase of collagen and fibronectin deposition, and, if it is, which crowder is the most efficient for that.

In order to reach the above-stated goal, the following objectives should be achieved:

- Assembly of the dermal scaffolds;
- Analysis of fibroblasts' viability in the dermal scaffolds in the presence of the crowders;
- Analysis of collagen type I and fibronectin deposition by fibroblasts in the dermal scaffolds in the presence of the crowders.

Ultimately, the development of this dissertation aims to contribute to the iSkin2 project by providing a better understanding regarding the impact of MMC effect in the studied substitute, while also providing advances to an increasingly studied subject which is MMC. This way, the work performed is expected to represent a small step towards the assembly of more efficient and clinically relevant skin substitutes among the immense work that has been done in this area.

1.3 Outline

The structure of this document is organized as follows:

- **Chapter 1: Introduction**

  This chapter comprises the context and motivation of this dissertation, while also presenting its objectives. The thesis structure is also described.

- **Chapter 2: Theoretical Concepts**

  In here, some theoretical notions considered important for the understanding of this work will be provided, namely concerning skin and MMC.

- **Chapter 3: State of the Art**

  This chapter provides a literature review of MMC-related works.

- **Chapter 4: Materials and Methods**

  This chapter describes the experimental procedure performed in this dissertation. Firstly, the methods for matrix production will be described, following cell culture description. Then, the methods for cellular viability assays and immunocytochemistry procedures will be assessed.

- **Chapter 5: Results and Discussion**

  In this chapter, the results obtained in this work and respective discussion will be displayed.

- **Chapter 6: Conclusions and Future Perspectives**

  This chapter summarizes the overall results obtained in this work and presents the principal conclusions retained from them. It also assesses to what extent the objectives proposed were achieved. Finally, some considerations will be provided for future works.

- **Appendices**

  This chapter provides additional content to literature review by showing a table summarizing the works in literature about MMC. It also provides several protocols followed during the experimental procedure, while also describing statistical considerations done in this work.

2

Theoretical Concepts

In this chapter, important theoretical concepts in the context of this dissertation will be addressed. Firstly, the definition of tissue engineering (TE) and its principles will be given. Secondly, some notions about skin constitution will be approached. Then, a brief idea about the wound healing process will be described. Next, some characteristics of the scaffold's materials and fabrication methods used in this dissertation will be described. Finally, important concepts about MMC will be explained.

2.1 Tissue Engineering Principles

TE is the field that aims to develop biological substitutes that restore, maintain or improve tissue function through the application of engineering and life sciences principles, being considered a subfield of regenerative medicine (RM) [2]. TE's techniques usually apply a combination of scaffolds, cells and growth factors for the formation of functional substitutes. This combination constitutes the fundamental triad of TE [3].

Scaffolds are structures that provide mechanical and chemical support to cells, acting similarly to an ECM. These can be obtained through diverse methods, namely by material manipulation through various fabrication techniques [3]. Section 2.4 gives a clearer insight about scaffolds and the characteristics of the materials and fabrication methods used in this dissertation.

Cell selection is also crucial depending on the tissue intended to be replaced. Regarding skin, differentiated cells like fibroblasts and keratinocytes, the most abundant cells in this type of tissue, are mostly used in skin substitutes. There can be single cell type approaches or multicellular approaches in substitute assembly. In section 2.2.2, a more profound introduction to these two cell types is given.

Growth factors are biologically secreted signaling molecules capable of, namely, promoting cell proliferation, cell migration, cell differentiation and wound healing. The implementation of growth factors in TE substitutes is very promising, namely by contributing to shorter production times [4]. Although the macromolecules used in the context of this dissertation as crowders are not considered growth factors, their utilization

serves the same final purpose, as they are expected to allow a faster and more accentuated cell growth and ECM formation. Section 2.5 encompasses a theoretical introduction to the MMC concepts.

In the context of this dissertation, the triad constitution is:

- **Cells:** Fibroblasts
- **Scaffolds:** PCL matrices, CS matrices, GEL matrices, and ternary/dermal matrices (combination of all the referred)
- **Growth factors:** None, but from the analogy stand point explained above, macromolecular crowders may have identical effects as growth factors

2.2 Skin

In this section, some important notions about the structure and constitution of skin are given.

2.2.1 Anatomy of Skin

Skin can be divided into two main layers: the epidermis and the dermis. The epidermis is a stratified, avascular, squamous epithelial tissue which assembles the outermost layer of skin, containing four or five sublayers. Its main function is to ensure the body's protection against external aggressions [5], [6].

The deeper, thickest layer of skin is the dermis, constituted of fibrous, filamentous, and amorphous connective tissue [6]. This layer is abundant in blood vessels, nerve endings and glands [7]. The dermis provides skin its elasticity and tensile strength, protects the body from mechanical injury, binds water, aids in thermal regulation, and includes receptors of sensory stimuli [6].

The hypodermis (subcutaneous tissue), although not being considering a layer of skin, is located beneath the dermis, and is constituted essentially of adipose tissue. Its functions are related to the formation of lipidic barriers [7]. The anatomical structure of skin is presented in Figure 2.1.

2.2.2 Skin Cells: Keratinocytes and Fibroblasts

The principal cells of epidermis are the keratinocytes. These cells undergo a differentiation process known as keratinization, as keratinocytes migrate from the basal layer to the surface of the epidermis, allowing a constant renewal of this layer or, in case of injury, its regeneration. Keratinization plays an important role in ensuring a physiological behavior of the epidermis [5], [6].

The principal active cells found in connective tissues are fibroblasts. These are dermis' main cells, whose function is to produce structural proteins of the ECM, namely collagen

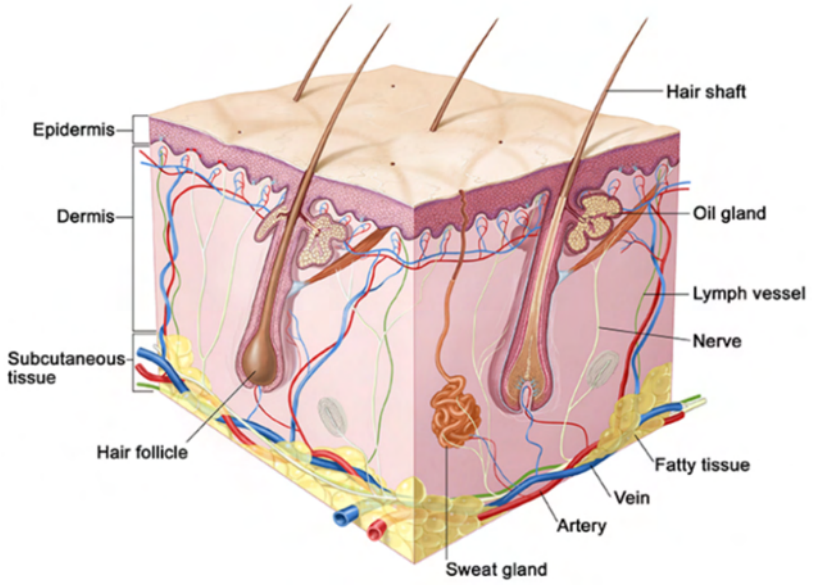

Figure 2.1: Anatomy of human skin. Reproduced from [8].

[5], [6]. Fibroblasts not only play an important role in the creation of novel ECM in injured tissues, but also in maintaining the ECM in uninjured tissues [9].

Fibroblasts and keratinocytes present major importance in the wound healing process in skin. These cells respond to inflammatory stimulus in case of injury, resulting in the enhancement of their proliferation, migration, and maturation. Additionally, the cross talk between these two cell types is one of the most relevant interactions for the repair/regeneration cascade in skin [10].

2.2.3 Extracellular Matrix

The ECM can be defined as a dynamic three-dimensional structure secreted by cells that provides mechanical and chemical support to the surrounding cells. ECM is composed of various macromolecules, usually highly concentrated, which interact with cells, generating signals via feedback loops in order to control their behavior and modulate various cellular events such as adhesion, migration, proliferation, differentiation, and synthesis. Cell fate is directly influenced by the signals provided by ECM, and the dysregulation of such interactions may result in pathophysiologies [11], [12]. ECM plays an important role in TERM as it protects and retains transplanted cells at the site of implantation, while also acting as a depot for bioactive molecules [13].

Usually, the macromolecules of the ECM are classified as fiber-forming, non-fiber-forming, and matricellular proteins. The first ones provide mechanical strength to the matrix forming a 3D framework of rigid proteins. In skin tissue, the most common fiber-forming protein is by far collagen (there are several types of collagens, namely collagen I, III, and IV), but many others such as elastin, laminin, fibronectin and fibrillin also participate in structure assembly. Secondly, non-fiber-forming molecules act mostly as chemical

mediators, functioning to form a charged, dynamic, and osmotically active space, while also filling the interstitial space created by the fiber-forming proteins. Glycosaminoglycans (GAG), such as hyaluronic acid (HA), are, along with proteoglycans, the main non fiber-forming macromolecules of skin [14]. Finally, unlike the other proteins, matricellular proteins can be absent in normal skin, however, they are expressed after skin injury [12], [15]. Figure 2.2 gives a schematic view of the mentioned components.

When the structure of the ECM is compromised, in case of injury, the normal wound healing process will ultimately result in the creation of new ECM. As mentioned before, fibroblasts play an important role in the formation and maintenance of ECM, however, the molecules synthetized are also extremely important in the regulation of fibroblasts' activity. This interaction can be seen as an autocrine regulation [15].

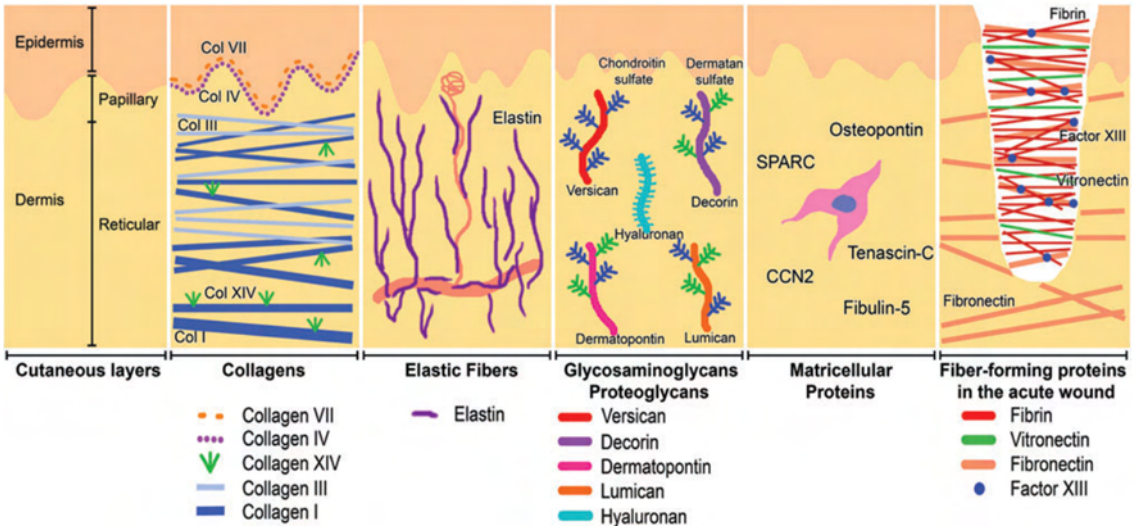

Figure 2.2: ECM of normal skin with various macromolecules and other structures indicated. Reproduced from [15].

2.3 Wound Healing

Following injury, skin integrity must be restored. This event unleashes a set of physiological reactions to ultimately restore the normal structure and function of skin. This process is designated wound healing. Wound healing can be summarized in four phases: hemostasis, inflammatory phase, proliferative phase, and tissue remodeling [16].

Briefly, the hemostasis consists in platelet activation, release of growth factors, aggregation and clot formation at the site of injury, preventing further blood loss and providing a temporary matrix for cellular migration. Then, the immune system promotes an inflammatory reaction, recruiting neutrophils, lymphocytes, and macrophages responsible for battling external agents and secreting growth factors. The proliferation phase is induced next with the accentuated migration and proliferation of fibroblasts, resulting in the production of matrix macromolecules and ECM, as well as the proliferation of keratinocytes.

Angiogenesis, granulation tissue formation and re-epithelization also occur. Lastly, the remodeling phase is responsible for the neo-dermis maturation, as granulation tissue gradually diminishes and skin components are remodeled, forming a functional tissue. One of the main alterations is the remodeling of type III collagen into type I collagen, which is further reorganized into parallel fibrils, contributing to the formation of a scarred tissue. The activity of matrix metalloproteinase (MMP)s, which are enzymes responsible for the degradation of several ECM proteins, is considerably enhanced in this stage. Failure in any of these stages compromises the wound healing process, possibly resulting in chronic wounds [10], [16], [17].

The gradual shift from an inflammatory to a proliferative response occurs due to the cellular interactions between fibroblasts and keratinocytes. Fibroblasts secrete paracrine factors, such as fibroblast growth factor (bFGF), keratinocyte growth factor (KGF), vascular endothelial growth factor A (VEGF-A) and insulin-like growth factor 1 (IGF-1), which communicate with adjacent keratinocytes. Keratinocytes release prestored interleukin 1 (IL1) which signals fibroblasts, promoting their production of KGF and, consequently, accentuating keratinocytes proliferation. Additionally, keratinocytes also produce other growth factors such as VEGF-A and platelet-derived growth factor (PDGF), which promote angiogenesis and fibroblasts' production of ECM. The inflammatory cells, such as macrophages, also play an important role in triggering proliferative responses in fibroblasts and keratinocytes through the release of transforming growth factor (TGF), such as TGF-β. This is responsible for the expression of myofibroblast phenotypes, which cause wound contraction and contributes to wound closure [10], [18]. Figure 2.3 shows a schematic view of the interactions described.

As explained, the activity of fibroblasts and keratinocytes (and their cross talk) is extremely important for wound healing. Providing adequate environments for these cells in skin substitutes using MMC can play an important role in improving fibroblasts and keratinocytes' function, namely by inducing a faster ECM deposition, which ultimately results in faster wound healing.

2.4 Scaffolds

In TE, scaffolds provide structural and chemical support for cell growth and, thus, ECM deposition. There has been intensive research in materials science with the ultimate objective of achieving the ideal scaffold for each type of tissue. Scaffolds' material, configuration and fabrication technique directly influence its efficacy. In this section, the characteristics of the polymers used in this dissertation will be discussed, as well as the fabrication method.

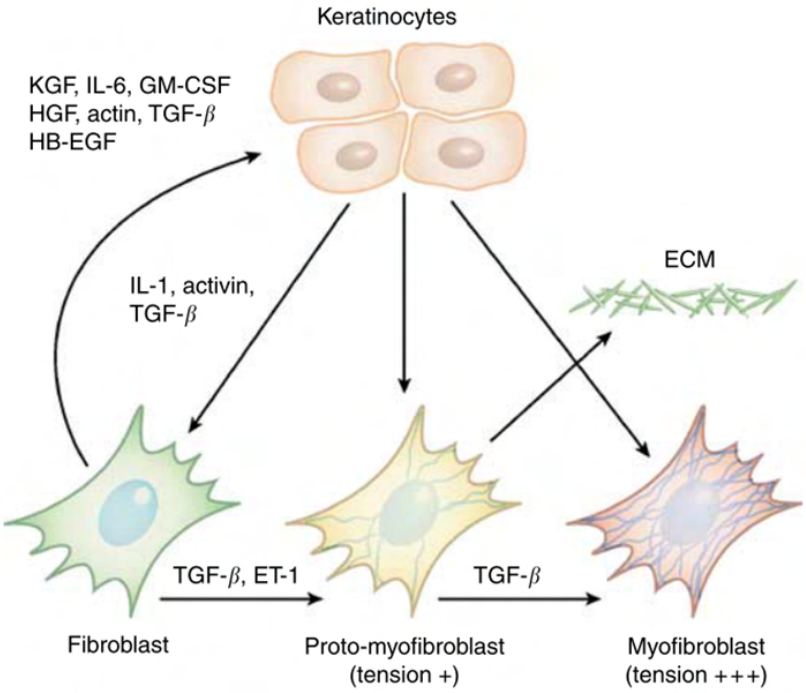

Figure 2.3: Interactions between fibroblasts and keratinocytes. Growth factors convey information between these two cell types and fibroblast differentiation into a myofibroblast phenotype. Reproduced from [18]

2.4.1 Materials

The dermal scaffold produced in this dissertation is composed of chitosan (CS), gelatin (GEL) and polycaprolactone (PCL). CS is a natural polysaccharide derived from chitin, which is the second most abundant biodegradable natural polymer. CS is frequently used as a scaffold in skin TE due to its high biocompatibility, high biodegradability, bacteriostatic effects, and hemostatic properties [19]. The most relevant property of CS regarding wound healing is its propensity to induce plentiful formation of granulation tissue with angiogenesis. Additionally, CS has been shown to induce fine collagen fibers histologically [20]. However, CS behaves as a polycation when dissolved in acidic solutions, and its solutions show high viscosity, even at low concentration, thwarting its processing through electrospinning [21], [22].

GEL is a biopolymer derived from the denaturation of collagen. It is more readily available and much cheaper than other ECM proteins, highly biocompatible and biodegradable, while also possessing a chemical structure very similar to collagen. When blended with CS, GEL facilitates CS's manipulation for the electrospinning process and, since both are extremely abundant and possess high biocompatibility and degradability, their association is promising in TE. [22], [23].

However, these two polymers still do not provide sufficient mechanical support, hence, PCL can be used to compensate this flaw. PCL is a synthetic, biodegradable, and biocompatible polyester, with great ability to be molded into different shapes. According to its

production method, different mechanical properties are achieved, therefore, PCL can be manipulated to provide high structural support to natural materials it is blended with [24].

2.4.2 Electrospinning

Electrospinning is the most used technique to produce fibrous scaffolds. This process consists in the application of high electrical voltage between a needle, connected to a syringe that contains the polymeric solution, and a collector linked to the electrical ground. The high voltage induces the continuous drawing of solution out of the needle into the collector. As the jet travels towards the collector, solvent evaporation and jet elongation lead to the deposition of polymeric fibers onto the collector. Electrospun fibrous scaffolds provide a nanostructure with interconnected pores, which mimics the ECM of natural tissues and promotes cell adhesion. Thus, electrospinning is one of the most well-established and recurrently used fabrication technique in TE [25], [26], and will be the fabrication method used in this dissertation.

2.5 Macromolecular Crowding

This section will first introduce the concepts related to MMC, providing a theoretical explanation of its biophysical consequences. Then, the characteristics and applications of the most recurrently used macromolecules will be described.

2.5.1 MMC concepts

The intracellular and extracellular environments in biological systems are crowded with a high number of molecular species, corresponding to a volume occupancy from 5 % up to 40 % [27]. In these conditions, despite an accentuated molecular packing, no single molecule is present at a predominantly high density, which differentiates the concepts of MMC and high concentration [28]. MMC effect can be described as the equilibria and kinetics of macromolecular reactions and interactions in highly volume-occupied or crowded conditions, such as most of physiological environments [29].

Excluded volume effect (EVE) enunciates that two molecules cannot occupy the same space at the same time, due to steric hindrance, electrostatic repulsion or chemical interactions [28]. In an environment with a greater volume of molecules, each molecule excludes other molecules from its vicinity, which is indicative of the correlation between MMC and EVE. The fraction of the total volume occupied by macromolecules is denoted as fractional volume occupancy (FVO), which in addition to the unavailable space in the vicinity of the molecules (caused by their electrostatic and steric interactions), comprise the excluded volume (see figure 2.4) [13], [28]. In a system with an increasing concentration of new molecules, the number of possible ways to add these molecules is reduced, due to the EVE: the available volume for molecules to be added is restricted to the space

that they are not excluded from [30]. The level of entropy of the system is affected by this phenomenon, as a space restriction indicates the reduction of the degree of disorder or randomness. As postulated in the second law of thermodynamics, any system has the tendency of maximizing its disorder and reducing its order. Therefore, by adding new molecules, although the excluded volume initially increases, the system will then react in the opposite direction by enhancing molecular association, resulting in the diminution of the excluded volume and in the restoration of some of the available volume that was lost by the presence of the molecule (figure 2.5) [28].

Diffusion is the fundamental molecule transportation form in living environments and is thought to also be directly influenced by MMC: diffusion rates decrease in the presence of MMC due to obstruction in molecular motion, which is influenced by several reactant's and crowder's physiochemical properties, namely viscosity, pH, size, among others [13], [28], [31].

In sum, MMC is a clear regulator of several biological processes, such as protein folding, enzymatic activity, or protein and DNA stability [28], [32]. In the context of this dissertation, though, it is important to highlight how MMC influences ECM formation and deposition: in highly crowded *in vivo* extracellular environments, the diffusion of procollagen (precursor to collagen), and N- and C- proteinases (enzymes) is restrained or prohibited, which culminates in accelerated procollagen conversion to collagen and, consequently, collagen assembly and ECM deposition [28].

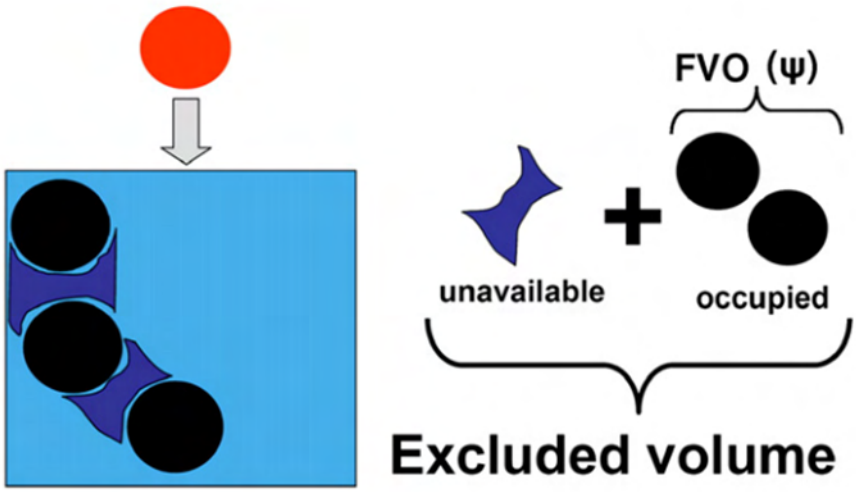

Figure 2.4: Excluded volume effect representation. The FVO can be calculated, while unavailable volumes are challenging to compute. Reproduced from [32]

MMC is an important characteristic in biological systems, and a needful requirement for life, as proteins and enzymes function in environments with great macromolecular abundance (e.g. proteins, polysaccharides, nucleic acids), as explained before. The extracellular concentration of body fluids and human tissues varies, respectively, between 37 g/l to >1000 g/l and 900 g/l to >2100 g/l. However, this highly crowded condition is

often despised in *in vitro* procedures, as cell culture media rarely present concentrations above 100 g/l [28]. Therefore, biochemical, and biological reactions *in vitro* are affected by such dilute and molecularly deprived conditions, diverging from what is achieved *in vivo*. Regarding the synthesis and deposition of collagen, such systems cause a very slow conversion of procollagen into collagen. This may occur due to the N- and C- proteinases deactivation before their action on procollagen, or due to the dissolution of procollagen (which is water-soluble) before its conversion to collagen (which is insoluble) [13], [28]. As a matter of comparison, this conversion may take less than 1 hour in physiological conditions [33], while *in vitro* it takes more than 3 days [34]. These attenuations may be at the origin of the difficulties regarding ECM formation in tissue engineered substitutes.

In sum, experts defend that it is impossible to expect physiological behavior from cells when they are embedded in such dilute (and non-physiological) culture media [28], resulting in recent increased efforts to understand this concept of MMC and to determine the most efficient macromolecules to crowd the media with.

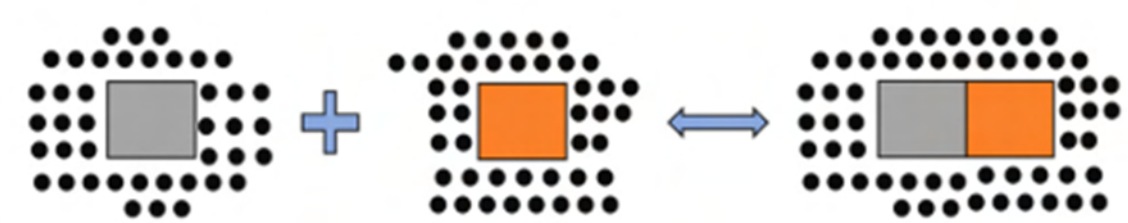

Figure 2.5: Illustration of the MMC effect. The increased crowding conditions induce molecular association. Reproduced from [28].

2.5.2 Macromolecules

The most reported macromolecular crowders are Ficoll (Fc), carrageenan (CR), dextran sulfate (DxS), polyvinylpyrrolidone (PVP) and hyaluronic acid (HA). The characteristics and properties of these macromolecules will be described next. Chapter 3 will give a clearer insight about the work reported in the literature with the molecules mentioned.

2.5.2.1 Ficoll

Fc is a neutral, nonionic, highly branched, hydrophilic polysaccharide that is extremely soluble in aqueous solutions. Fc is usually utilized as a density gradient medium for the separation and isolation of eurakyotic cells [35], and is also one of the most utilized macromolecules in MMC studies.

2.5.2.2 Dextran Sulfate

DxS is a natural, biocompatible, hydrophilic, biodegradable and negatively charged polysaccharide. It has a wide range of applications, often being used as an additive in cell cultures to act as an anti-coagulant. It is also used as an anti-inflammatory and

anti-aging agent in cosmetics, while also having anti-viral properties [36]. DxS has also been studied as a macromolecular crowding agent due to its anionic properties.

2.5.2.3 Polyvinylpyrrolidone

PVP is a synthetic polymer with a vast use in the pharmaceutical industry and in medicine, as it possesses excellent biocompatibility, can form stable associations with many active substances and is cost effective. PVP is also water-soluble, nontoxic, chemically inert, temperature-resistant, pH-stable and non-ionic. Its solubility confers a great range of applications since PVP is soluble in several solvents, as it possesses both hydrophilic and hydrophobic functional groups. An important drawback of PVP is its low biodegradability. In TE, PVP is usually used as a biomaterial for scaffold production, however, recent studies showed its potential use as a macromolecular crowder, as it will be furtherly discussed [37], [38].

2.5.2.4 Hyaluronic Acid

HA is a large, anionic, non-sulphated GAG present in the ECM of epithelial and connective tissues and a biodegradable polymer. HA plays a role in production, assembly and organization of ECM, helps in the growth of epithelial cells, and is essential in wound healing and scar formation. It is soluble in water, has an overall net negative charge and interacts with molecules in its vicinity via both steric and electrostatic repulsion, which has led to recent reports using HA as a macromolecular crowder. HA also has anti-aging or anti-inflammatory applications, as well as other applications in TE [39], [40].

2.5.2.5 Carrageenan

CR is a negatively charged natural high molecular weight sulphated polysaccharide obtained by extraction from red seaweeds. CR possesses interesting biological and chemical properties for TERM, such as anticoagulant, antiinflammatory, antioxidant, antitumour and antiviral properties. Additionally, CR is also used in pharmaceuticals, drug release and food industries. Seaweeds are a rich source of sulphated polysaccharides, with the likes of fucoidan, fucan, galactan and ulvan also being mentioned to have such applications. However, CR has some drawbacks and adverse effects on biological systems, as the sulfate group has been associated with adverse effects towards blood coagulations and immune system activation, with studies on animals suggesting that the long-term use of CR promotes the development of pathologies such as ulcers or tumour growth. Regarding its use as a macromolecular crowder *in vitro*, several recent studies point out CR as the optimal crowding agent to promote ECM deposition, as it will be discussed further [41], [42].

3

State of the Art

In this chapter, a literature review is presented. Initially, the applications of TE in skin and its limitations are discussed, consequently addressing how MMC emerges as a solution for some limitations. Then, a review of the MMC-related efforts present in the literature are given. Finally, the conclusions summarize the most important points identified in the studies analyzed, which are taken in consideration in the development of this thesis.

3.1 Literature Review

For this review, several studies, from the beginnings of TE in skin, to the most recent efforts regarding MMC, are considered.

3.1.1 Tissue Engineering in Skin and Current Limitations

TE applied to skin regeneration has had a considerable development in the last 30 years, with the emerging of several game changing techniques and products. In the 1980s, even before TE was a well-defined area, Yannas and Burke created Integra™ [43], the first skin substitute introduced in the clinic, which dramatically increased the survival rate of patients with extensive burn injuries. Since then, TE has experienced tremendous advances, culminating in the development of various novel skin substitutes with clinical potential, having epidermal, dermal, or even dermal-epidermal application, with the use of allogenic or autologous cells. Nowadays, commercially available dermal-epidermal substitutes using autologous cells like Permaderm™, Tiscover™, denovoSkin™, PolyActive or TissueTech Autograft System, utilize extracted fibroblasts and keratinocytes cultured in appropriate conditions to simulate the bi-layered structure of skin [44]. Figure 3.1 illustrates the differences between the TissueTech Autograft System, which incorporates several layers in a single susbtitute, including keratinocyte and fibroblast layers, and Integra™, a simpler acellular system. Even though each skin substitute has its own advantages and applications, they still fail to fully mimic natural skin, and the fact that autografting remains the gold standard in clinic is elucidative of the limitations of these

products [45]. Reduced vascularization, poor mechanical properties, scarring, and immune rejection constitute important drawbacks of the available substitutes. Additionally, the expensiveness of such substitutes, the inability to produce differentiated structures like glands and hair, and the need for a time-consuming process of 2-3 weeks of cell culture for their production are indicators of the need for further investigation [44], [46].

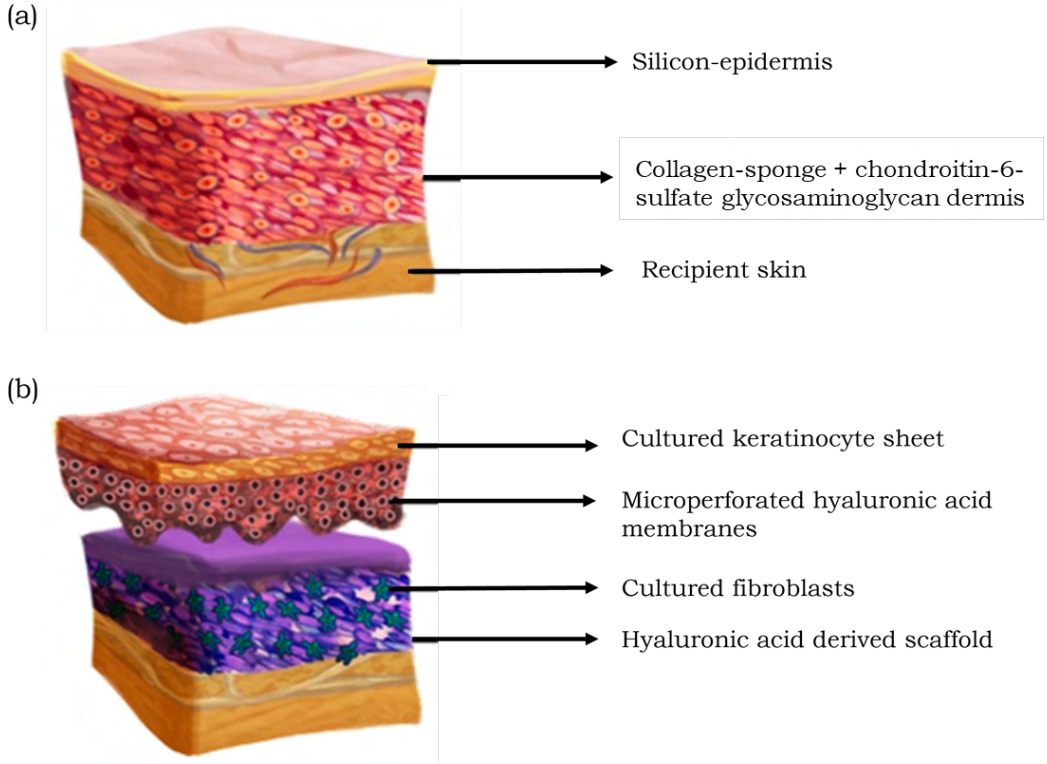

Figure 3.1: Constitution of skin substitutes. (a) Integra; (b) TissueTech Autograft System. Adapted from [44].

3.1.2 MMC as a New Solution

MMC emerges in TE in an attempt to overcome the limitations referred above, especially to significantly reduce the production time of engineered substitutes. As a matter of fact, the typical development of ECM-rich 3D constructs requires prolonged *in vitro* cultures. Per example, for the production of an ECM-rich implantable device for skin, 14 days are needed in single layered approaches, while 50 days is the time needed to produce a skin substitute with full thickness [28]. Several biophysical, biochemical or biological approaches have been experimented with the objective of promoting faster production times, such as mechanical stimulation, oxygen tension and growth factors, alone or in combination. However, none seems to significantly promote a faster and enhanced production of ECM, which is an extremely limiting factor for the development of efficient substitutes, given the crucial role ECM plays in cell fate [28]. The implementation of MMC principles is expected to help filling this gap.

The concept of MMC has been known for decades, with reports underlining its biological importance dating back to the early 1990s [29], [47]. However, the first studies applying its principles in TE were only published in 2007 [48], [49].

3.1.3 Initial Studies with MMC: Ficoll and DxS as Crowders

Lareu *et al.* in 2007 were the first to assess the potential of MMC in cell culture and TE. In [48], lung fibroblasts were cultured under several crowding conditions (500 kDa DxS and 10 kDa DxS at 100 µg/ml; 200 kDa polysodium-4-styrene sulfonate (PSS) at 100 µg/ml; Fc 70 and Fc 400 at 50 mg/ml) and seeded onto Biobrane or PLLA scaffolds. Collagen deposition was significantly increased under PSS and 500 kDa DxS crowding, with a 36-fold and 23-fold increase above control levels (2 days of culture without any crowding supplementation), respectively. These results corroborate a preliminary study conducted by the same author [49], as DxS seems to be a determinant factor in the enhancement of collagen deposition. DxS and PSS, which are negatively charged macromolecules, seemed to outperform neutral macromolecules (Fc). The authors defend that this is because negative molecules possess a higher hydrodynamic radius, which is a parameter that describes the effective size of a macromolecule in a physiological environment. Per example, although 500 kDa DxS and 400 kDa Fc have similar molecular weights, the negative molecule has a greater hydrodynamic radius, and hence greater FVO percentage, at a 500 times lower concentration. As procollagen is a negatively charged molecule, electrostatic repulsion resulting from the interaction with other negatively charged macromolecules induces a higher EVE and, thus, greater procollagen conversion to collagen. Regarding fibronectin, there was no enhanced deposition. Another interesting achievement in this study is related to ECM deposition directly into the supporting materials, as ECM footprints revealed relevant amounts of collagen in the scaffolds after detergent removal of the cells, which is indicative of the potential of MMC in approaches using decellularized matrices.

Soon-after, MMC was also applied with the objective of providing an *in vitro* model to study the pathophysiology of fibrosis ('Scar-in-a-Jar') [50]. Lung fibroblasts were cultured under distinct crowding conditions, with the results suggesting that the use of MMC allowed the complete biosynthetic cascade of collagen matrix formation, including complete conversion of procollagen into collagen, its extracellular deposition and lysyl oxidase-mediated crosslinking. Moreover, this study showed that it is possible to control, in accordance with the desired system, collagen matrix deposition rate and morphology. On the one hand, to achieve a rapid deposition (2 days), negatively charged crowders should be used (DxS). On the other hand, crowding the mixture with neutral mixed Fc served as the accelerated mode, with doubling of the collagen deposition achieved at the sixth day post-culture.

Zeiger *et al.* [51] studied the effect of MMC in human bone-marrow mesenchymal stem cells (MSC) utilizing a Fc 70/400 cocktail, concluding that such supplementation promoted an increase in the assembly of collagen types I and IV, while also inducing the

alignment of ECM fibers. Another important conclusion taken from this article is that seeding the cells together with MMC is beneficial for both cell proliferation and ECM deposition, in comparison to a 24h post-seeding crowding.

Fc and DxS were the first relevant crowders reported in the literature showing promising results. Actually, Fc utilization has prevailed along the years, being one of the most highly regarded macromolecular crowders. Figure 3.2 is representative of the capability of Fc supplementation to increase the deposition of various ECM proteins.

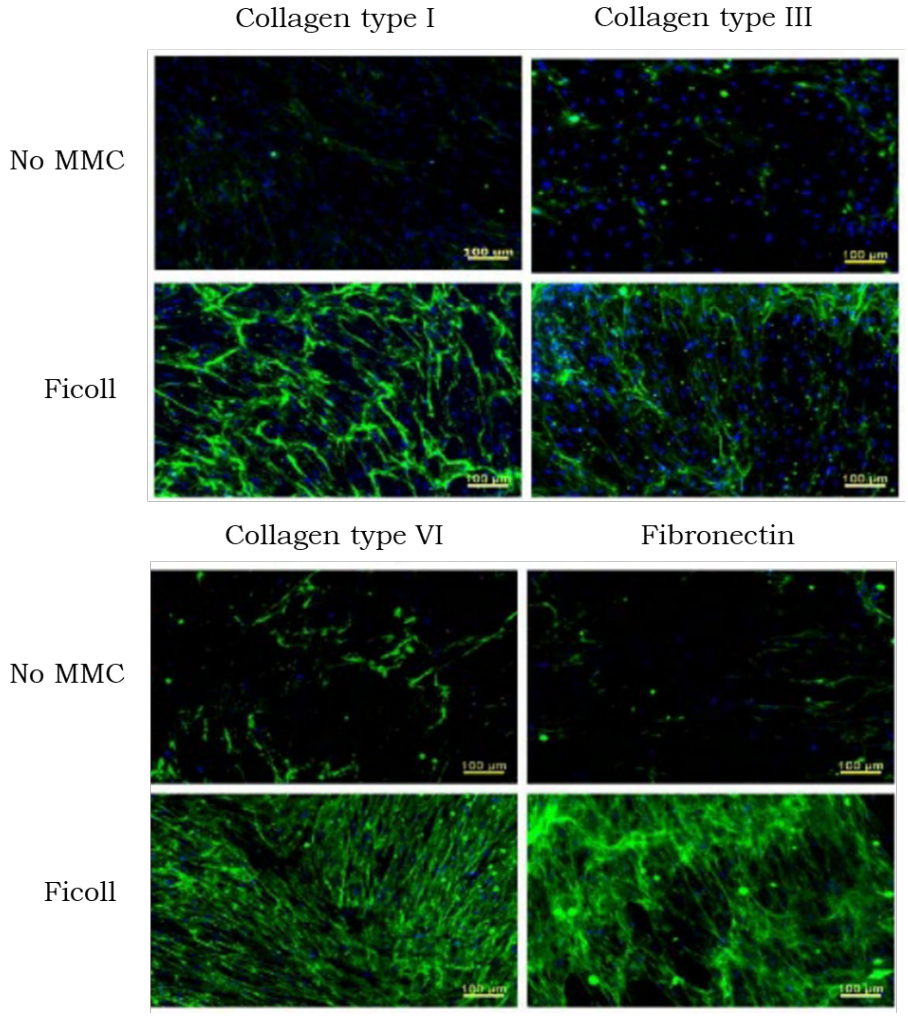

Figure 3.2: Immunocytochemistry analysis shows significantly increased deposition of several ECM proteins under Fc supplementation by human corneal fibroblasts, in comparison to non-crowded conditions. Images were obtained after 2 days of culture. Reproduced from [52].

3.1.4 Hyaluronic Acid as a Crowder

Shendi *et al.* [39] reports the first use of HA as a macromolecular crowder using human neonatal fibroblasts. However, the results did not show significant increase in ECM gene expression nor deposition. These outcomes were contradicted by Garnica-Galvez *et al.*

[53] studies, where the effectiveness of HA as a crowder in adipose-derived stem cell-cultures and its physicochemical properties were assessed. HA enhanced the deposition of collagen III and collagen IV in comparison to non-MMC groups, however, it still did not come close to CR and Fc performances. The authors finish by stating that, unless a biological benefit for HA is identified, the use of Fc and CR over HA should be prioritized for enhanced and accelerated ECM deposition.

3.1.5 Polyvinylpyrrolidone as a Crowder

Rashid *et al.* [38] reports the first evaluation of the use of PVP as a crowder, establishing a comparison with Fc mixtures in human dermal fibroblast and human bone-marrow MSCs cultures. Different concentrations of PVP 360 kDa, PVP 40 kDa, and Fc cocktail were analysed. The best results regarding collagen types I and IV and fibronectin deposition with PVP 40kDa were achieved using 18% FVO, as with PVP 360kDa, these were obtained at a FVO of 54%. Viscosity of the crowders was also assessed: solution's viscosity increases with an increasing concentration of crowders. While for PVP solutions the increase is linear, for Fc mixtures the increase is exponential. For the optimal FVO percentage of each crowder, the viscosity levels associated to these crowding conditions were between the physiological ranges, which indicates the possibility of the use of PVP in TE and *in vivo*.

In sum, Fc mixtures at 9% and 18 % FVO still outperformed, with the curiosity of 9% FVO outperforming 18% FVO, which is more commonly used in literature, any PVP used. However, due to the high cost and the limited FVO ranges with physiological viscosities of Fc, PVP could present a good alternative to Fc.

3.1.6 Carrageenan as a Crowder

More recently, CR has emerged in the literature with significant impact, with several publications referring it as the most efficient crowder [28], [42], [54], [55].

Gaspar *et al.* [55] assessed the influence of biophysical properties of macromolecular crowders, such as polydispersity and charge, in ECM deposition in human dermal fibroblast culture. Several concentrations and molecular weights of CR, Fc and DxS were studied, as well as Fc and DxS cocktails. Results showed that CR, DxS 100 kDa, and DxS 500 kDa significantly enhanced ECM deposition, with CR appearing to be the most effective. Fc, due to its neutral charge, did not match the enhanced ECM deposition of the negatively charged crowders. Mixed crowding, utilizing Fc and DxS cocktails, enabled higher polydispersity, however, only DxS cocktails managed to achieve similar performance (but still inferior) to CR, as Figure 3.3 shows. This indicates that high polydispersity and negative charge are biophysical characteristics capable of promoting a more efficient EVE by the crowders and, thus, inducing an accelerated rate of biological reactions, which explains the efficiency of CR.

Satyam *et al.* [54] also performed comparative studies between Fc 70/400 mixtures, DxS and CR in order to assess the most efficient crowder in several cell types. CR outperformed all the remaining crowders, with the authors hypothesising that its inherent high molecular polydispersity was the key modulator of excluded volume, inducing greater ECM deposition. Figure 3.4, obtained from this report, shows how effective CR supplementation is to enhance ECM deposition in comparison to non-crowded groups.

Given the effectiveness of CR, it would be interesting to assess if other molecules derived from the same seaweeds showed similar results. De Pieri *et al.* [42] evaluated the biophysical properties of different seaweed polysaccharides, such as arabinogalactan, fucoidan, galactofucan, ulvan and CR, and their effect on human adipose derived stem cell cultures. None of the crowders, except arabinogalactan, affected celular viability. Fucoidan, galactofucan and ulvan promoted an enhanced ECM deposition, especially collagen type I and type V, however, they still did not match CR efficiency. This work opens new possibilities for the use of other polysaccharides derived from seaweeds, but reinforces the influence of CR in MMC-related studies.

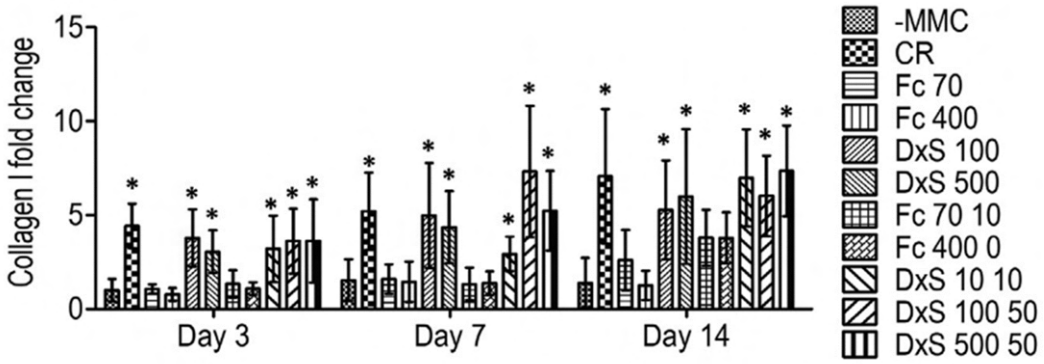

Figure 3.3: SDS Page and densitometric analysis revealed that, in human dermal fibroblast cultures, DxS and, especially, CR induced the highest collagen type I deposition among all the considered crowders. Statistically significant differences ($p < 0.01$) to uncrowded groups are marked with *. Reproduced from [55].

3.1.7 MMC and Oxygen Tension Combination

Oxygen tension is an essencial signal that regulates developmental processes, cell fate and tissue function, with its extracellular concentration flucuating between 0.5% and 14% within an organ, depending on how far the cells are located from capillaries. Each tissue and cell type needs specific oxygen levels, which has led to research efforts to optimize oxygen supplementation in cell cultures and TE [56]. Combinating oxygen tension with MMC could enhance the pretended effects, with several reports exploring this hypothesis.

Cigognini *et al.* [57] demonstrated that CR significantly enhances ECM deposition in human bone marrow MSC at both 20% and 2% oxygen tension. In another study, Satyam *et al.* [56] assessed the simultaneous effect of oxygen tension, foetal bovine serum (FBS) concentration and MMC (75 µg/ml CR) in human dermal fibroblast culture. Results show

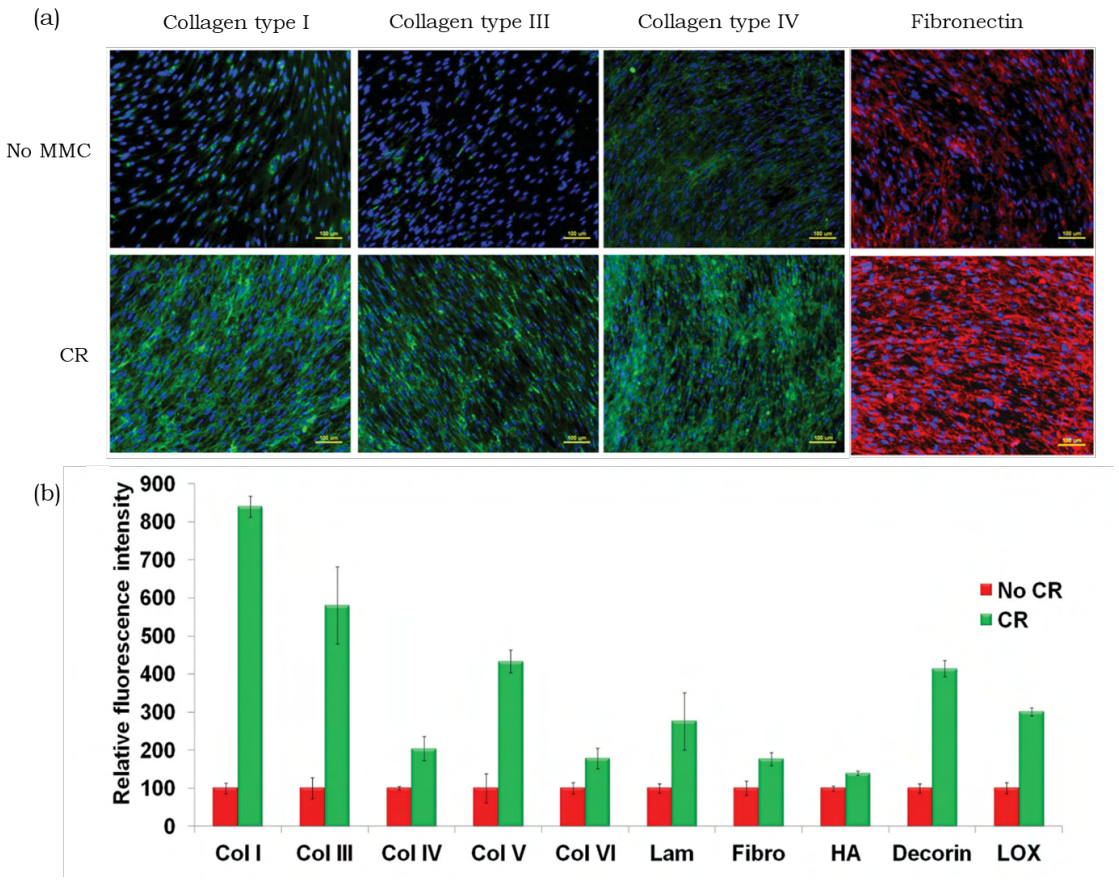

Figure 3.4: Supplementation with CR drastically increases deposition of several ECM proteins after 2 days. (a) Immunocytochemistry analysis and (b) relative fluorescence intensity measurements confirmed higher deposition for all the proteins analysed, with the more accentuated increase being achieved in collagen type I and III. Reproduced from [54].

that the presence of CR enhances ECM deposition in all time points (3, 7 and 14 days), and in all oxygen tensions and FBS concentrations. Additionally, 2% oxygen tension was associated to an increased ECM deposition, in comparison to 0.2% or 20%, at all time points, at all FBS concentrations and in the presence or absence of crowder. FBS concentration of 0.5% also seemed to outperform 10% FBS. More recently, Kumar *et al.* [58] performed similar studies in human corneal fibroblasts, with the highest ECM deposition being achieved after 14 days under 2% oxygen tension, at 0.5% serum concentration and crowded with 75 µg/ml CR.

In sum, these studies suggest that MMC and oxygen tension, individually or associated, can be crucial microenvironment modulators for faster development of TE substitutes.

3.1.8 MMC and Growth Factor Combination

Similarly to what can be achieved between oxygen tension and MMC, combining growth factors with MMC can also be beneficial in TE. Tsiapalis *et al.* [59] reports the simultaneous use of MMC and growth factors (IGF-1, PDGFββ, GDF5, TGFβ3) in tenocyte cultures. CR supplementation induced higher collagen deposition in comparison to non-crowded conditions or with/without any growth factor and, when supplemented together with TGFβ3, induced even more collagen deposition. TGFβ3 outperformed the remaining growth factors. This comparison between MMC and growth factors shows just how effective CR is, as it outperforms supplementation with natural occurring substances in the physiological environment. This data suggests that crowders combined with growth factors could also play an important role improving engineered constructs.

3.1.9 MMC in 2D and 3D Models

Most of the investigation performed about MMC is in two-dimensional models, in a monolayer of cultured cells. As a matter of fact, of all the articles reunited for this review, only four of them mention the use of scaffolds (three-dimensional models) [48], [60]–[62]. Chen *et al.* [60] work established a comparison between 2D and 3D models, using porcine chondrocytes and Fc 70/400 cocktail. Regarding cells grown in 2D, the results corroborate previous findings, namely the enhancement of collagen type II deposition and GAGs production, in the presence of MMC. However, in a 3D model, the supplementation with MMC did not enhance matrix deposition and maturation. In fact, evidences of deterioration of the quality of the engineered cartilage were observed. The authors propose that this could be because, among other reasons, the support matrix already confers a packed environment and, by adding even more crowding, matrix degradation enzymes, which inhibit ECM formation, are activated.

Other reports present opposite results. Cámara-Torres *et al.* [61] studied the use of Dx and Fc in human MSCs seeded in 3D additive manufactured scaffolds, with the results showing that both crowders supported cellular viability, and allowed increased ECM production and mineralization. Tsiapalis *et al.* [62] studied the effect of CR supplementation in tenocytes seeded in Biosyn™ scaffolds, showing that MMC enhanced and accelerated ECM deposition onto the construct.

These findings provide the notion that MMC could have distinct effects in 2D and 3D environments, and that the potential of MMC in 3D models is still not clear.

3.1.10 MMC to Produce Dermal-Epidermal Junction

When it comes to the assembly of bi-layered skin substitutes, it is of great importance to assure the development of a functional dermal-epidermal junction (DEJ). Benny *et al.* [31] reported the use of mixed MMC, consisting of a mixture of Fc 70 and Fc 400, in monocultures and co-cultures of fibroblasts and keratinocytes to assess the production

of an interlinked membrane of ECM, characteristic of the DEJ. The resulting ECM was enriched with collagen I and IV, fibronectin and laminin 5. More importantly, the deposition of collagen VII, the anchoring fibril component of the DEJ, was also enhanced. Moreover, the results suggest that fibroblasts are the major cellular contributors to the DEJ, rather than keratinocytes, as they induce greater collagen VII deposition and act as a promotor of collagen VII production and deposition by keratinocytes. MMC was the key factor in achieving these results in a significantly reduced time frame.

3.1.11 MMC to Produce Decellularized ECM-rich Matrices

Wong *et al.* [63] showed good results in implementing MMC (Fc 70/400 cocktail) in the assembly of an acellular dermal fibroblast ECM. This ECM had an enhanced deposition of collagen type I and type IV, and fibronectin. The matrix was then utilized to expand keratinocytes, being crucial in the modulation of keratinocyte growth and differentiation.

Another study by Satyam *et al.* [64] also reports the use of Fc 70/400 cocktail in the assembly of fibroblast-derived decellularized matrices, which allows *in vitro* proliferation and differentiation of podocytes. This platform displays abundance in growth factors and molecules, enabling podocyte maturation. Such publications are indicative of the utility of MMC in the assembly of decellularized ECM-matrices, as it promotes an accelerated and efficient ECM production by the removed cells.

3.2 Conclusions

The implementation of MMC in TE is a clear step-forward in the direction of producing more efficient substitutes. In Appendix A, a table summarizing the academic work regarding MMC is provided.

The following points represent important suggestions, limitations or characteristics denoted during this analysis:

- Negatively charged crowders, especially CR, seem to be the most effective
- Fc 70/400 mixture, although neutrally charged, has achieved good results
- Seeding cells together with MMC is more effective than seeding the cells and only adding the crowders the following day
- MMC in three-dimensional models is still a very unstudied topic
- Efficiency in the production and deposition of collagen and fibronectin may differ for the same crowder
- Combinating MMC with growth factor supplementation or oxygen tension may offer even better results

This dissertation tries to take in consideration the maximum number of these topics in order to achieve the intended results.

4

Materials and Methods

In this chapter, the experimental procedure for the development of this work is described. First, the materials and methods utilized for the production of the CS, GEL, PCL and ternary matrices are shown. Then, we present the approach used regarding fibroblast cell culture, where the macromolecular crowders were utilized. Further, cellular viability tests with resazurin assays are shown. Finally, immunocytochemistry procedures are described, as well as the process for fluorescence image acquisition and analysis.

It is important to note that a cycle of work is constituted by the following points:

1. Produce the matrices.
2. Carry out cell culture.
3. Perform resazurin assays and analyze them.
4. Perform immunocytochemistry staining.
5. Analyze the immunocytochemistry staining images and assess ECM deposition.

However, many precursory studies which led to the definition of a well-established procedure were also performed, which are also described along the following sections.

4.1 Matrix Production

For the assembly of the dermal scaffold, electrospinning was performed. The matrices were either constituted by one of the polymers (unitary matrix) or by the association of the three polymers (ternary matrix). In total, four different types of matrices were produced: GEL matrix, CS matrix, PCL matrix and ternary matrix. The procedure for the fabrication of these scaffolds will be described next.

Table 4.1: Polymers used for matrix production.

Polymers	MW (kDa)	Supplier
CS	500	Cognis
GEL from cold water fish skin	n.i.	Sigma-Aldrich
PCL	80	Sigma-Aldrich
PEO	2000	Sigma-Aldrich

Table 4.2: Reagents used for matrix production.

Reagents	Chemical Composition	MW (Da)	Supplier
Acetic Acid, Glacial	$C_2H_4O_2$	60.05	Thermo Fisher
GTA 50 %	$C_5H_8O_2$	100.1	Merck
Distilled Water	H_2O	18.02	-

Table 4.3: Polymer concentration (expressed in percentage of polymer mass relative to total solution mass) and solvent composition (given by the ratio of the masses of acetic acid and distilled water) of the solutions used in this work.

Solution (w/w)	PCL	CS	GEL	PEO	Acetic Acid : H_2O
PCL	20	0	0	0	100:0
CS	0	2	0	0.4	90:10
GEL	0	0	25	0	90:10
Ternary	2	2	2	0.2	90:10

4.1.1 Materials and Reagents

Table 4.1 provides the molecular weight (MW) and the supplier of the various polymers used for matrix assembly. Table 4.2 describes the characteristics of the reagents used in matrix production.

4.1.2 Solution Preparation

Table 4.3 summarizes the concentrations used to produce the solutions for electrospinning. These concentrations have been studied and optimized in preceding work done in the Tissue Engineering Group [65]. A combination of glacial acetic acid and distilled water constituted the solvent in CS, GEL and ternary solutions, while in the PCL solution the solvent was 100% acetic acid. As described in [65], high molecular weight poly(ethylene oxide) (PEO) was added to solutions containing CS in order to overcome the adversities related to the electrospinning process of these solutions, due to their high conductivity and CS's cationic behavior.

The solutions were prepared and placed in the magnetic stirrer (MS-H-Pro, Scaninst) overnight. For PCL solutions, if the polymer was not dissolved properly, an ultrasonic cleaner (UD100SH-3L, Eumax) was used.

4.1.3 Electrospinning

The matrices were assembled using a rotating electrospinning setup (figure 4.1). Additional translational movements were implemented to provide a more uniform distribution of the fibers through the aluminium sheet (collector). All the solutions were processed equally, connecting a 5 ml syringe with the solution to a 23-gauge needle. Electrospinning was then performed using a high voltage power supply (T1CP300304p, ISEG) providing a voltage of 18 kV. The rate used was of 0.3 mL/h, and 3.5 mL of the solution was dispensed. The tip of the needle was at a distance of 25 cm from the collector.

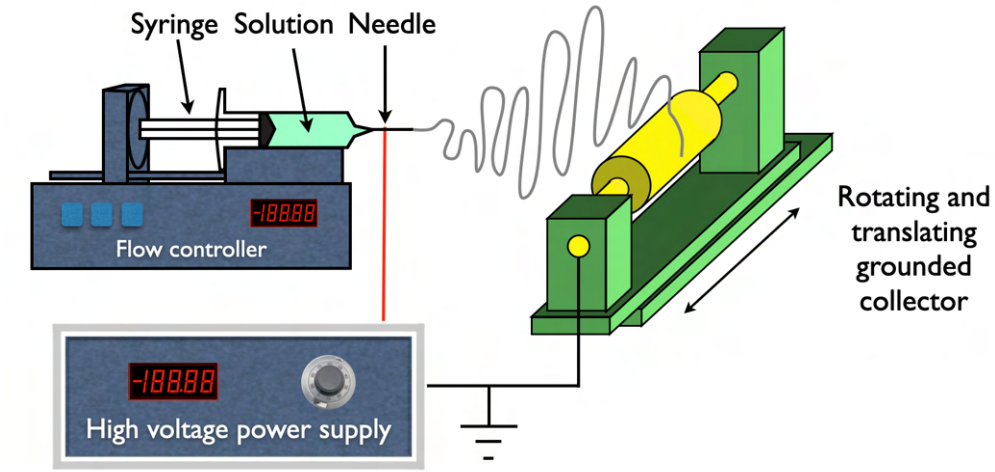

Figure 4.1: Electrospinning technique illustration.

4.1.4 Crosslinking

Matrices containing GEL and CS need crosslinking to be an effective scaffolding structure, since these polymers dissolve in water at room temperature [65]. GEL, CS and ternary matrices were crosslinked by being exposed to glutaraldehyde (GTA) vapour: an open recipient containing a 50 wt% GTA solution in water and containing scaffolds was placed in a hermetically sealed container, in order to expose the matrices to an atmosphere saturated with GTA vapour. This container was placed in an oven at 37 ºC for 3 hours. Then, the scaffolds were kept in a vacuum desiccator for three days to remove any residual absorbed GTA.

4.2 Cell Culture

After matrix production, cell cultures were performed, where MMC was incorporated. This section comprises the procedures done in this ambit. First, the preparation of scaffolds and crowders for cell culture is described. Then, the different culture studies performed will be explained.

Table 4.4: Reagents used for cell culture.

Reagents	Supplier
DMEM low glucose	BioWest
Ethanol (70% v/v)	Home-made
TrypLE™ express	Gibco
Trypan blue stain (0.04%)	Gibco
FBS	Biowest
Penicillin (100 U/ml)	Invitrogen
Streptomycin (100 µg/ml)	Invitrogen
PBS	Home-made
Ascorbic Acid	Alfa Aesar
Fc 70 kDa	GE Healthcare
Fc 400 kDa	GE Healthcare
PVP 55 kDa	Sigma-Aldrich

4.2.1 Materials and Reagents

Table 4.4 provides the reagents and respective suppliers used during cell culture procedures described in this section.

The following equipment was used: centrifuge (K3 Series, Centurion Scientific), CO_2 incubator (MCO-19AIC, Sanyo), hemocytometer (Bürker, Hirschmann), microscope (Eclipse Ti-S, Nikon), biological safety cabinet (E-series, Labculture), deep freezer (Cryocell), waterbath (Memmert). All the instruments used during such experiments were sterile and non-pyrogenic in order to avoid cell culture contamination.

4.2.2 Matrix Preparation

The scaffolds produced as descibed in 4.1 were cut into 12 mm diameter disks utilizing punch-holes. Matrices were then sterilized with ethanol v/v 70% for 20 minutes and washed 3 times with phosphate buffered saline (PBS). Glycine was then used to neutralize non-reacting aldehyde groups (given their toxicity) of matrices that were crosskinked. Before cell culture, the matrices were washed once more with PBS. Protocol B.1 was followed.

4.2.3 Crowder Preparation

Two different crowders were utilized in this dissertation: Fc and PVP.

4.2.3.1 Preparation of Ficoll

Fc mixtures were prepared by utilizing Fc 70 kDa at a concentration of 37.5 mg/mL and Fc 400 kDa at a concentration of 25 mg/mL dissolved in low glucose Dulbecco's modified Eagle's medium (DMEM) supplemented with 1% penicillin/streptomycin (Pen Strep) and 10% foetal bovine serum (FBS), with associated FVO of 18%, as it is the most used/efficient Fc mixture described in the literature.

Before application in cell culture, the crowders were sterilized. Thus, the solution with the crowder was filter-sterilized utilizing 0.22 µm filters. The solution was kept at 4 ºC.

4.2.3.2 Preparation of Polyvinylpyrrolidone

PVP 55 kDa was also studied as a crowder. Since the literature only reports the use of PVP 40 kDa and PVP 360 kDa, it was necessary to assess the intended concentration of PVP 55 kDa to achieve a FVO of 18%. Rashid et al. [38] showed that a FVO of 18% produced the highest collagen production in crowding conditions with PVP 40 kDa and, considering that PVP 55 kDa possesses a similar molecular weight to PVP 40 kDa or, at least, more similar in comparison with the other studied MW (360 kDa), a FVO of 18% was selected to be used in this work.

To calculate the concentration of PVP 55 kDa associated to a FVO of 18%, the protocol described in [38] was followed. Equation 4.2 was obtained to determine the concentration to be used. The volume of each macromolecule (V) was calculated using equation 4.1, with PVP 55 kDa having a hydrodynamic radius of R_H=5.65 nm [66].

$$V = \frac{4}{3}\pi R_H^3 \tag{4.1}$$

$$\frac{m}{V_T} = \frac{FVO}{100\%} \times \frac{MW}{6.023 \times 10^{23} \times V} \tag{4.2}$$

The concentration obtained was m/V_T = 21.76 mg/mL. Thus, PVP 55 kDa was dissolved in low glucose DMEM supplemented with 1% Pen Strep and 10% FBS at a concentration of 21.76 mg/mL. The sterilization was performed in the same way as for Fc mixtures. The solution was kept at 4ºC.

4.2.4 Cell Culture

Human caucasian foetal foreskin fibroblasts (HFFF2) (see figure 4.2) were cultured in T75 or T25 flasks with DMEM low glucose supplemented with 10% FBS and 1% Pen Strep and maintained in a incubator with a humidified 5% CO_2 atmosphere at 37 ºC.

4.2.4.1 Cell Culture for Crowder Optimization

Preliminary studies were performed in order to:

- Assess the influence of seeding cells together with MMC-supplemented medium or supplementing the cells with MMC only 24 hours post-seeding;
- Assess the influence of supplementing cell medium with L-ascorbic acid 2-phosphate (AA);

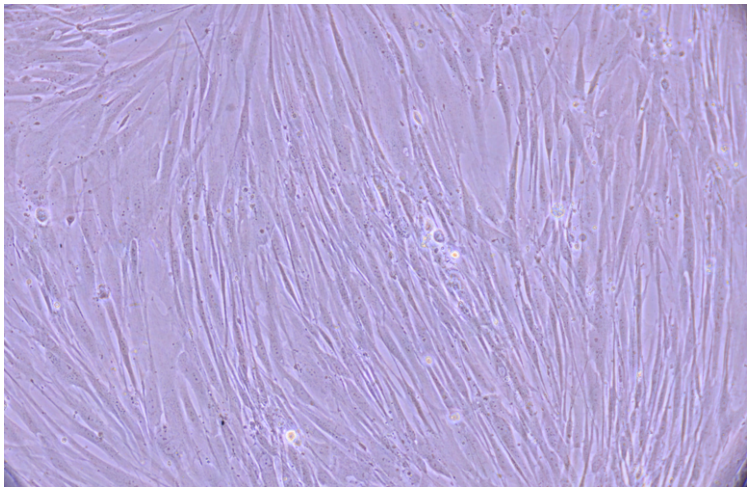

Figure 4.2: Microscope image of HFFF2 cells. Magnification of 100x was used.

- Perform immunocytochemistry optimization studies.

For this, HFFF2 were cultivated for 7 days in 24-well culture plates. Cells were seeded at a density of 50000 cells/well (25000 cells/cm^2) onto coverslips placed in the bottom of each well following protocol B.2. Six different culture conditions were assessed as following:

- Standard medium: low glucose DMEM with 10% FBS and 1% Pen Strep (DMEM);
- Supplementation with AA (DMEM + AA);
- Supplementation with MMC (MMC);
- Supplementation with MMC and AA (MMC + AA);
- Supplementation with MMC 24-hours post seeding (MMC 24h);
- Supplementation with MMC 24-hours post seeding and AA (MMC 24h + AA).

For MMC conditions, Fc cocktail as described in 4.2.3.1 was used. AA at 100 µM was added to MMC or DMEM solutions. In conditions where MMC was only added 24 hours post-seeding, the cells were initially seeded with DMEM. AA supplementation was performed right at day 0. Conditions containing AA had their medium changed every day, while the remaining were changed every 2 days. In every condition, the amount of culture medium used was 1 mL/well. The plates were kept in 37 ºC, 5% CO_2 conditions. All the samples were fixed at day 7.

4.2.4.2 Cell Culture in Gelatin, Chitosan and Ternary Matrices

The auto-fluorescence of CS and GEL can impair the visualization of cells and ECM proteins through immunocytochemistry assays. Thus, preliminary cultures were performed

with adjustments in the fluorescent staining protocol in order to assess the possibility of performing immunocytochemistry assays in these mats.

HFFF2 were seeded in the GEL, CS or ternary mats that were placed inside home-made Teflon inserts with an internal area of 0.5 cm^2, at a concentration of 12500 cells per insert, according to protocol B.2, and cultured for 7 days. MMC supplementation was performed right at day 0. 250 µl of culture medium, with or without MMC, was added to each Teflon insert and changed every two days. The plates were kept in 37 ºC, 5% CO_2 conditions. All the samples were fixed at day 7.

4.2.4.3 Cell Culture in PCL Matrices

HFFF2 were cultured for 7 days in 24-well culture plates, similarly as described in CS, GEL and ternary matrices. In total, four different conditions were used for each crowder studied: +MMC in PCL matrix, +MMC in coverslips, -MMC in PCL and -MMC in coverslips. Samples were fixed at each time point (3, 5 and 7 days). The plates were kept in 37 ºC, 5% CO_2 conditions.

4.3 Cellular Viability

To assess the viability of the seeded cells, and to determine if MMC would have any detrimental effect on cells, resazurin assays were performed.

4.3.1 Materials and Reagents

Culture medium as described earlier and resazurin (Alfa Aesar) at 0.04 mg/ml in PBS were used in this phase of the work.

4.3.2 Resazurin Assay

Fibroblast viability in the different crowding conditions (with or without MMC) and in the different supporting materials (coverslip or PCL matrix) was assessed via resazurin assays performed at each time point (day 3, 5 and 7 post-seeding), according to protocol B.3.

4.3.3 Analysis of Results

The data obtained at each time point was analyzed using Microsoft Excel. The optical density (OD) difference between 570 nm and 600 nm wavelengths for each well was calculated, as presented in equation 4.3. The final OD value for each condition was assessed by calculating the mean of the values of all the wells corresponding to that condition, and subtracting the average OD value of the resazurin control group, as in equation 4.4.

$$OD_{dif} = OD_{570nm} - OD_{600nm} \tag{4.3}$$

$$OD_{condition} = \overline{OD_{difsamples}} - \overline{OD_{resazurincontrol}} \tag{4.4}$$

The uncertainty of the absorbance data was calculated through the law of propagation of uncertainty. Experimental standard deviation of each condition and control group was calculated, with the uncertainty of the final OD value of each condition being given by equation 4.5.

Statistical significance was assessed via t-tests as described in appendix C.

$$u^2_{c(OD_{condition})} = s^2_{m(OD_{condition})} - s^2_{m(OD_{resazurincontrol})} \tag{4.5}$$

4.4 Immunocytochemistry

In this section, the optimized immunocytochemistry procedure will be provided, as well as the optimization process. Additionally, the methods to study ECM deposition, from image acquisiton to ECM quantification will be described.

4.4.1 Materials and Reagents

Table 4.5 shows the reagents used during this phase of the work. The solutions produced for the development of these experiments are presented in table 4.6. The staining agents used were:

1. **Primary Antibodies**
    - Rabbit Anti-Collagen type I, Rockland 600-401-103-0,1
    - Mouse monoclonal $IgG_1\lambda$ Anti-Collagen type I Alpha 2 (COL1A2), Santa Cruz SC-393573
    - Mouse monoclonal $IgG_1\kappa$ Anti-Fibronectin, Santa Cruz SC-8422
2. **Secondary Antibodies**
    - Mouse IgGκ light chain binding protein (m-IgGκ BP) conjugated to CruzFluor™ 555, Santa Cruz SC-516177
    - Mouse IgGλ light chain binding protein (m-IgGλ BP) conjugated to CruzFluor™ 555, Santa Cruz SC-516191
    - Mouse IgGλ light chain binding protein (m-IgGλ BP) conjugated to CruzFluor™ 488, Santa Cruz SC-516190
    - Goat Anti-rabbit Alexa Fluor 488 conjugated, Elabscience E-AB-1055
3. **Other Fluorescent Stains**

Table 4.5: Reagents used during immunocytochemistry procedures.

Reagents	Supplier
Albumin, Bovine	Amresco
Glucose	n.i.
Triton X-100	Sigma-Aldrich
PBS	Homemade
PFA	AppliChem Panreac
Mowiol	Sigma-Aldrich
Glycerol	VWR

Table 4.6: Solutions used during immunocytochemistry procedures.

Solution	Composition
4% PFA	4% PFA in PBS
Fixing Solution	4% PFA with glucose at 40 mg/mL
Fixing Permeabilization Solution	Fixing solution with 0.1% Triton
2% BSA Solution	2% Bovine Serum Albumin in PBS
Mowiol	10% Mowiol, 25% glycerol, 15% H_2O, 50% Tris-HCl (0.2M, pH 8.5)

- Acti-stain™ 488 Fluorescent Phalloidin, Cytoskeleton, Inc.
- Acti-stain™ 555 Fluorescent Phalloidin, Cytoskeleton, Inc.
- DAPI Nucleic Acid Stain, Invitrogen™

4.4.2 Optimized Immunocytochemistry Protocol

For immunocytochemistry analysis, protocols in section B.4 were followed. Cells were washed with PBS, permeabilised with 0.1% Triton in fixing solution and fixed in 4% paraformaldehyde (PFA) supplemented with glucose at 40 mg/mL, at each time point (3, 5 and 7 days). Non-specific sites were blocked with 2% bovine serum albumin (BSA) in PBS for 1 hour at room temperature.

Cells were incubated overnight at 4 ºC with primary antibodies for collagen type I (Rockland 600-401-103-0,1) and fibronectin (Santa Cruz SC-8422) at 1:50 dilution. Secondary antibodies, goat anti-rabbit AF488 conjugated (Elabscience E-AB-1055) at 1:100 dilution (for collagen type I) and mouse IgGκ light chain binding protein, Santa Cruz SC-516177, at 1:50 dilution (for fibronectin), were incubated for 1h30 at room temperature. Cell nuclei were counterstained with 4% 4',6-diamidino-2-phenylindole (DAPI) in 2% BSA for 5 minutes.

Slides were mounted with 10 µl of Mowiol. Images of the samples were acquired using an epi-fluorescence microscope (Nikon Eclipse Ti) with a magnification of 400x, and then analysed with the ImageJ software, as described in subsection 4.4.4.

4.4.3 Optimization of Immunocytochemistry Protocol

To reach the above-described protocol, precursory studies had to be performed, since several difficulties were experienced along the work to obtain the desired images. The protocols in section B.4 were followed as well, but different antibody conditions were experimented, as described ahead.

Firstly, to make a comparison between the available red secondary antibodies, primary antibodies anti-fibronectin SC-8422 and anti-collagen type I Alpha 2 SC-393573 at 1:50 dilution were incubated in different samples. The secondary antibodies used were fibronectin anti-mouse IgG kappa, SC-516177, and collagen anti-mouse IgG lambda, SC-516191, both at 1:50 dilution. Acti-stain™ 488 Fluorescent Phalloidin was also incubated for 1h30 together with the secondary antibodies at 1:500 dilution to visualize actin filaments.

The two available primary collagen antibodies were also compared. For that, mouse collagen type I alpha 2 SC-393573 (COL1A2) and rabbit collagen type I (Rockland 600-401-103-0,1) were incubated at 1:50 dilution in different samples. Then, secondary antibodies were added to the respective primary antibodies: anti-mouse IgG lambda, SC-516190, at 1:50 dilution and goat anti-rabbit AF488 conjugated (Elabscience E-AB-1055). Acti-stain™ 555 Fluorescent Phalloidin was also incubated for 1h30 together with the secondary antibodies at 1:500 dilution.

After this procedure, the antibodies to be used for the remaining immunocytochemistry experiments were defined, as stated in section 4.4.2.

4.4.4 Study of ECM Deposition

After incubation of the samples with the antibodies, these were visualized in an inverted microscope. After the images were acquired, ECM deposition was quantified. In the next subsections, the processes of image acquisition and of ECM deposition quantification are explained.

4.4.4.1 Image Acquisition and Treatment

The samples were visualized using an epi-fluorescence microscope (Eclipse Ti-S, Nikon) with a digital camera (D610, Nikon). Camera Control Pro version 2 was the software used to acquire the images. For each channel, different exposure times and neutral filters were used, as presented in table 4.7. Unless otherwise mentioned, these were the parameters for image acquisition.

4.4.4.2 Nuclei Counting

Nuclei counting was performed to normalize the quantification of ECM deposition. Since it is expected that images containing a higher number of cells also contain more ECM, dividing the mean intensity of each image by the number of counted nuclei in the same

Table 4.7: Exposure time and microscope filter usage in fluorescence image acquisition of collagen, fibronectin and cell nuclei.

	Channel	Exposure Time	Neutral Filters
Collagen	Green	1/2 sec	Both
Fibronectin	Red	1/6 sec	Both
Nuclei	Blue	1/4 sec	None

image would allow to establish a comparison between images with different cell density. Accordingly, the main factor for higher or lower ECM deposition would not be the number of cells, but possibly the use of MMC or different scaffolds.

To count the nuclei, ImageJ was used and protocol B.4.4 as described in [67] was followed. Figure 4.3 shows the initial image obtained from the fluorescence microscope (a) and the image post-processing from which the nuclei counting is performed (b).

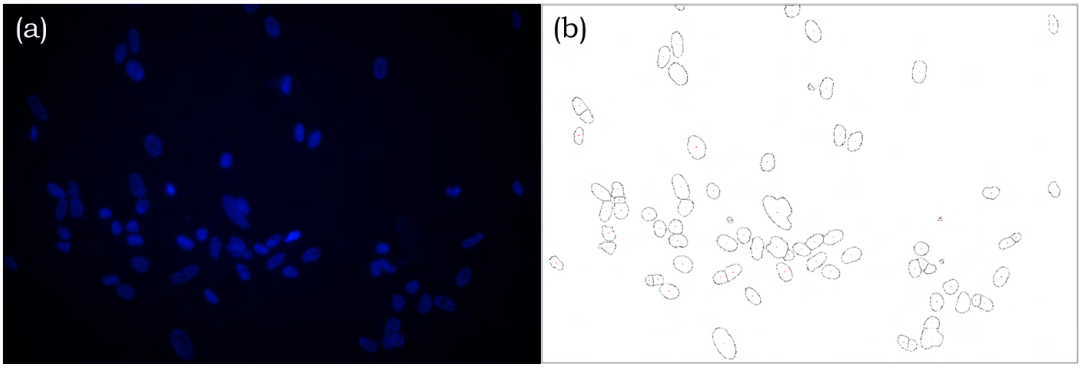

Figure 4.3: Image processing for nuclei counting. (a) Fluorescence image before processing; (b) Image used for nuclei counting after processing.

4.4.4.3 ECM Quantification

To establish an estimation of the amount of collagen or fibronectin deposited in each image obtained from immunocytochemistry, ImageJ was used. For each fibronectin or collagen staining image, mean gray value (MGV) was measured, which indicates the image's average intensity. Then, for each image, the MGV of at least three areas corresponding to the background were measured and averaged, providing an estimation of the background intensity of each image. This value was then subtracted from the image MGV, allowing to make a correction to the useful intensity for ECM quantification by removing the background intensity. Finally, this value was divided by the number of counted nuclei in the image, providing a value of MGV per cell (see equation 4.6), which is the normalized relative intensity measure used to compare the ECM deposition of the various conditions.

$$\text{MGV/Cell} = \frac{\text{Image MGV} - \text{Average MGV}_{\text{Background}}}{\text{Number of Nuclei}} \tag{4.6}$$

For each condition studied, the average of MGVs per cell were obtained from all the corresponding images, and their respective standard deviations. Statistical significance was assessed via t-tests as described in appendix C.

5

Results and Discussion

This chapter comprises the results obtained in this dissertation and their discussion. It is organized in five sections, with the first two presenting and discussing the results regarding the optimization of the immunocytochemistry procedure and of the crowder optimization cultures. Then, the results obtained in CS, GEL and ternary matrices will be discussed. Moreover, cellular viability assays will be presented and discussed. Finally, the results concerning the MMC effect in ECM deposition in PCL matrices will be discussed.

5.1 Immunocytochemistry Optimization

It was of great importance to perform initial studies where various antibodies were tested, since obtaining an efficient staining and, thus, good ECM deposition visualization was an indispensable requirement for the development of this work.

Firstly, the available antibodies for fibronectin and collagen red staining were tested as described in section 4.4.3. Figure 5.1 shows a comparison of the immunocytochemistry images obtained with these two available red staining agents. Foremost, it is important to note that the images, for both fibronectin and collagen, correspond to the same culture condition (with MMC), which allows a more adequate comparison. By analysing the images, both fibronectin and collagen appear to be stained by the respective antibodies, however, some differences can be observed: fibronectin staining appears to be more noticeable in comparison with collagen staining. This could be due to the presence of a higher amount of fibronectin than collagen in the respective samples, as fibronectin and collagen may not be produced equally by the cells, which is unlikely since collagen type I is the most abundant protein in the ECM. However, since it is expected that samples with higher cell concentration produce more ECM, and considering that the sample associated with collagen staining has a higher cell concentration, it would be expected that collagen staining presented higher intensity, which is not verified. Therefore, this difference in intensity could be associated not to the actual amount of protein deposited, but to the staining process. Additionally, only the alpha 2 chains of collagen type 1 are stained, when it is intended to stain the collagen type 1 protein as a whole, which of course affects

the intensity of the image.

A good method to evaluate the presence of non-specific binding is the utilization of primary antibody controls, which consists in merely incubating the secondary antibodies, with no previous application of primary antibodies. This ensures that staining is produced from the antigen detection by the primary antibody, and not due to unspecific binding [68]. Therefore, it is expected that the images acquired with these controls are mostly dark. The second row of images in figure 5.1 were obtained after performing this procedure. It is evident that non-specific bindings occur in the image related to collagen staining, while a way more darker image is obtained for the fibronectin staining, which indicates that the collagen staining process with the secondary antibody used is quite unspecific. Considering all this, fibronectin staining in the remaining work was performed using these antibodies (Mouse Anti-Fibronectin SC-8422 at 1:50 concentration + Anti-mouse SC-516177 [red] at 1:50 concentration). It was also necessary to test other antibodies for collagen staining.

For a more convenient experiment, it would be useful that collagen staining was carried out with green fluorescence, so that, for the same sample, blue, green and red stainings were all done, showing, respectively, nuclei, collagen and fibronectin. For that, two combination of primary + secondary antibodies were tested, as described in section 4.4.3. It is important to point out that one of the primary antibodies only bound to alpha 2 chains present in collagen type I (labeled as COL1A2 from now on), while the other primary antibody bound to collagen type I protein as a whole (labeled as COL1 from now on). Obviously, this work intended the visualization of collagen type I protein, not just the alpha 2 chains, so it would be expected that COL1 antibody was more adequate in comparison with COL1A2 for our purposes. However, studies were still performed to assess the staining by each antibody, with the results being shown in figure 5.2. By performing a similar analysis as before, it is evident that COL1A2 staining is nearly null, while COL1 staining achieves the expected outcomes. The fact that COL1A2 staining is reduced has to be related to the green secondary antibody efficacy, since in figure 5.1, where the red secondary antibody was utilized, it is possible to visualize fibronectin staining. It is also relevant to stress that primary antibody controls (only incubating the secondary antibody) were actually as awaited in COL1 staining, since the image is almost completely dark, which again ensures that non-specific bindings did not occur. As for COL1A2, the primary antibody control image is quite similar to the image with primary and secondary antibody incubation, which is indicative of the inefficiency of this staining process. With this being said, collagen type I staining in the remaining work was performed using these antibodies: Rabbit Anti-Collagen type I, Rockland 600-401-103-0,1 at 1:50 dilution + Elabscience goat anti-rabbit AF488 conjugated [green] at 1:100 dilution.

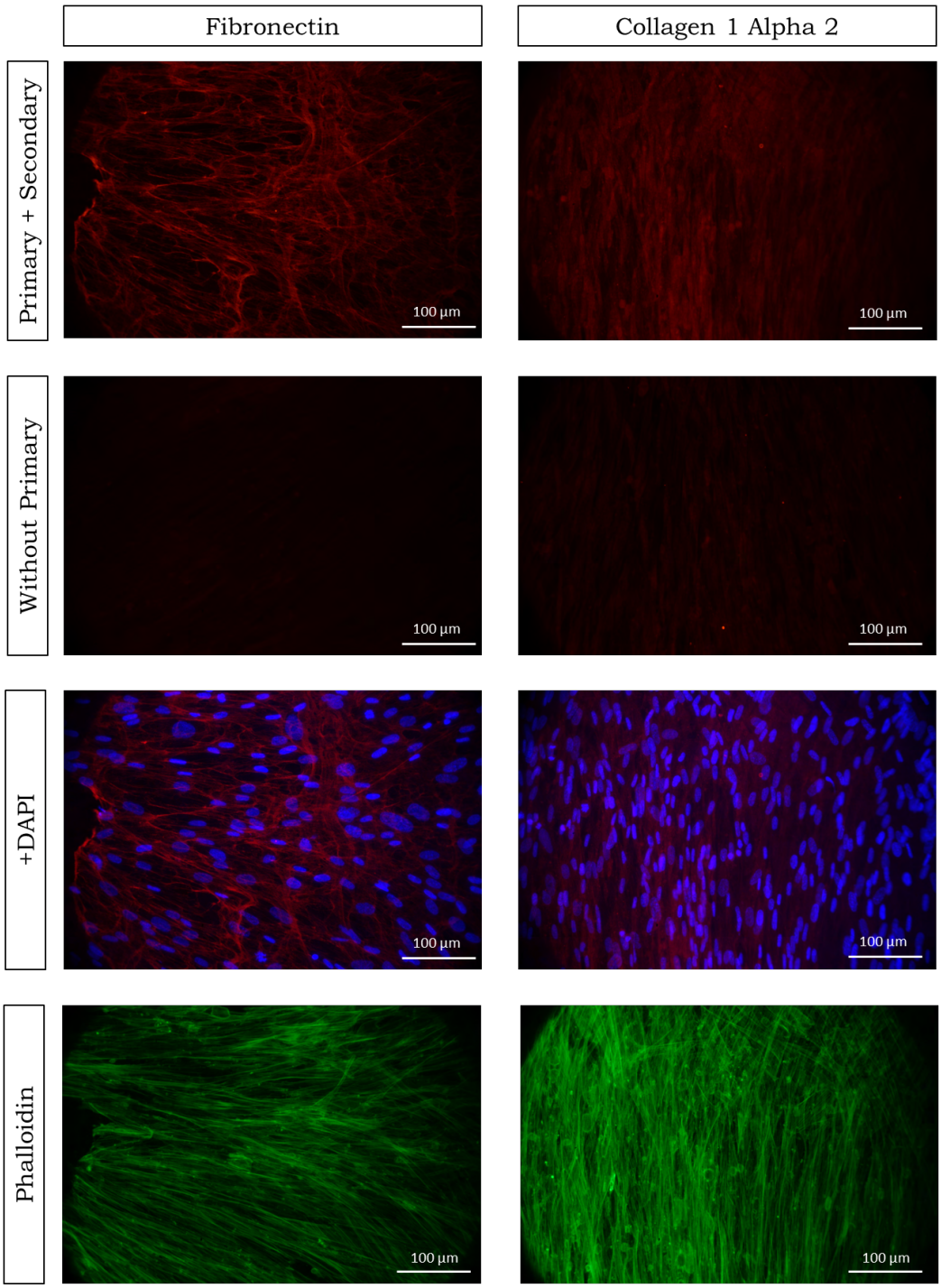

Figure 5.1: Comparison of fibronectin and collagen type I alpha 2 red staining in optimization studies. For each protein, an image is shown with the primary and secondary antibodies used, an image without the use of primary antibody (primary antibody control), and a composite image with nuclei and protein staining. Additionally, phalloidin staining of the given samples is also shown. All cultures were performed under the same crowding condition (Fc). Nuclei, fibronectin, collagen, and phalloidin images obtained with an exposure time of 1/4 seconds, 1 second, 1 second and 1/2 seconds, respectively. All the images were obtained with a 40x objective.

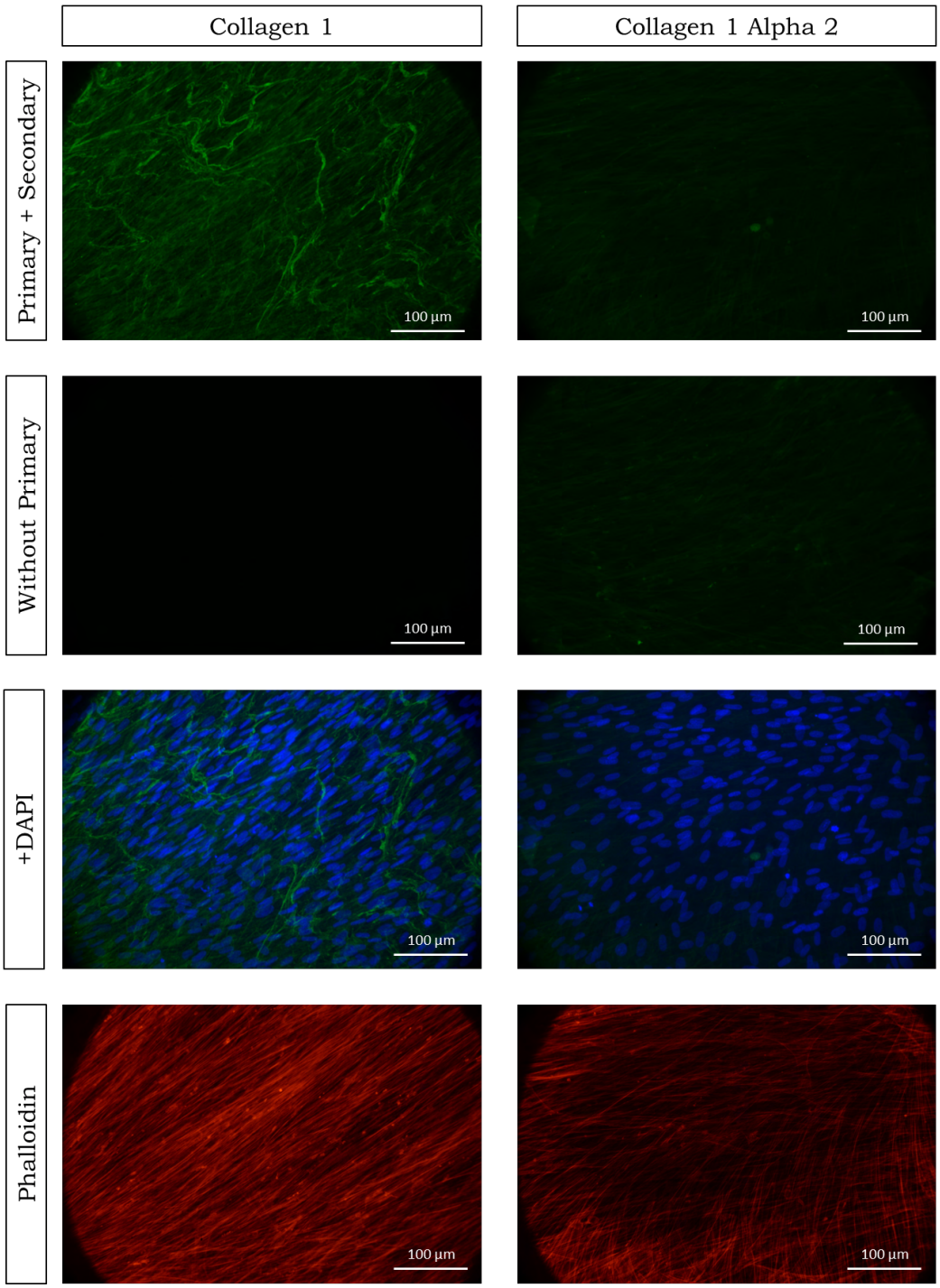

Figure 5.2: Comparison of collagen type I and collagen type I alpha 2 green staining in optimization studies. The presented images follow the same description as in figure 5.1. All cultures were performed under the same crowding condition (Fc implemented 24 hours post seeding). Nuclei, collagen and phalloidin images obtained with an exposure time of 1/4 seconds, 1/2 seconds and 1 second, respectively. All the images were obtained with a 40x objective.

5.2 Crowding Optimization

Figure 5.3 shows the images obtained for collagen type I and nuclei staining after crowding optimization cultures, after 7 days of culture. As one can observe, collagen type I deposition occurred in all conditions. Fibronectin deposition also occurred in all conditions, as can be observed in figure 5.4.

These cultures were performed with the objective of determining if any of the conditions allowed a greater ECM deposition, and understand if it would be useful to perform AA supplementation or only introduce crowders 24 hours post-seeding. However, through direct image visualization, it is difficult to assess if any relevant differences occurred. Actually, collagen type I and fibronectin deposition seems to be similar in all the conditions, and directly proportional to the number of cells. The reduction of cell density in such assays could enable an easier direct perception of an increase or decrease in the deposition of these proteins.

Having this in consideration, to complement this direct analysis, intensity measurements of the images present in figures 5.3 and 5.4 were performed. Figure 5.5 displays a relative amount of collagen deposition (a) and fibronectin deposition (b) in each condition, given by MGV per cell. Since there was only one sample for each condition, these results have no statistical significance, yet they still provide a more analytical approach to analyze collagen and fibronectin deposition, complementing image visualization.

Regarding collagen deposition, some differences in the intensity of the images of each condition are observed. For instance, MMC groups did not seem to consistently enhance collagen deposition in comparison to DMEM groups, especially when MMC was implemented 24 hours post-seeding. Only MMC groups with AA supplementation showed a slight increase in collagen deposition, with the remaining groups supplemented with AA not showing any improvement in this ambit.

Analyzing the intensity graph corresponding to fibronectin images, MMC groups actually seem to significantly increase fibronectin deposition. Again, using MMC only on the day after cell seeding does not seem to enhance fibronectin deposition, while the use of AA has distinct outcomes depending on the culture medium used.

Considering the above stated observations, for further work, AA supplementation was not performed, since these results were not clear about its effects. Even though AA utilization is very common in studies regarding MMC, we chose not to use it since the main focus of this work is to study the MMC effect by itself. Therefore, reducing the implementation of other factors could help to better assess the impact of MMC. Moreover, the implementation of MMC only 24 hours post-seeding did not seem to increase collagen nor fibronectin deposition and, since the reports in literature suggest that introducing MMC together with cells at seeding is more effective than only adding MMC on the following day (as discussed in chapter 3), the remaining work was performed introducing MMC right at day 0. Since it is expected that MMC has an immediate effect in cell metabolism, only using it 24 hours post-seeding would be inconsistent with all the

evidences. However, to reach more significant conclusions regarding the effects of using AA and only implementing MMC in the day following cell seeding, more studies should be conducted.

5.3 Autofluorescence in Chitosan and Gelatin Scaffolds

One of the main objectives of this dissertation would be to address ECM deposition by fibroblasts in the dermal scaffold, which is composed by GEL, CS and PCL, via immunocytochemistry. It is important to consider that, alike non-specific antibody binding, high autofluorescence of tissues or materials could present an important obstacle to the efficient immunocytochemistry procedure, as it makes discerning the background noise from the specific binding challenging. As a matter of fact, all tissues have autofluorescence to a certain degree, which may not be an impediment for immunocytochemistry. GEL is mentioned in literature to have an emission profile along the visible spectrum [69]. Pure CS is not referred as a polymer with high autofluorescence.

By observing figure 5.6, one can note the existence of an intense background in the green and red channels, especially in ternary and GEL matrices. CS matrices, although also presenting autofluorescence, show less background intensity. Overall, collagen and fibronectin visualization is impracticable in any of the mentioned matrices. Regarding the blue channel, nuclei visualization is possible as the background intensity is quite reduced in CS and GEL matrices, only seeming to increase in ternary matrices, but still allowing decent nuclei visualization.

Despite the inherent fluorescence of these materials, other factors such as the use of chemical cross-linkers for cell fixation can contribute to increased autofluorescence. A consequence of using aldehydes as fixing agents (in this work, PFA is used) is that their combination with amines forms Schiff bases, which results in an increased autofluorescence of the matrix [70]. Actually, Hu *et al.* [71] defends that although pure CS does not present autofluorescence, CS cross-linked with GTA becomes autofluorescent. To assess if the use of PFA could be the root of the autofluorescence problem, other fixation methods without PFA were tested. However, matrices containing GEL and CS were still cross-linked using GTA.

On the one hand, samples were immersed in 0.1% sodium borohydride solution in PBS for 5 minutes after fixing and permeabilization, as this treatment is reported to help dealing with autofluorescence problems, namely by removing aldehyde groups [72]. On the other hand, methanol fixing at -20ºC for 20 minutes was also tested as an alternative to formaldehyde fixing.

However, these alterations did not improve the fluorescence images obtained, with the high autofluorescence still not allowing to perform an adequate analysis or quantification of collagen or fibronectin deposition. No images were saved, as they were similar to those in figure 5.6. Future immunocytochemistry studies should be performed considering alternatives to the crosslinking method used, since it is very likely that

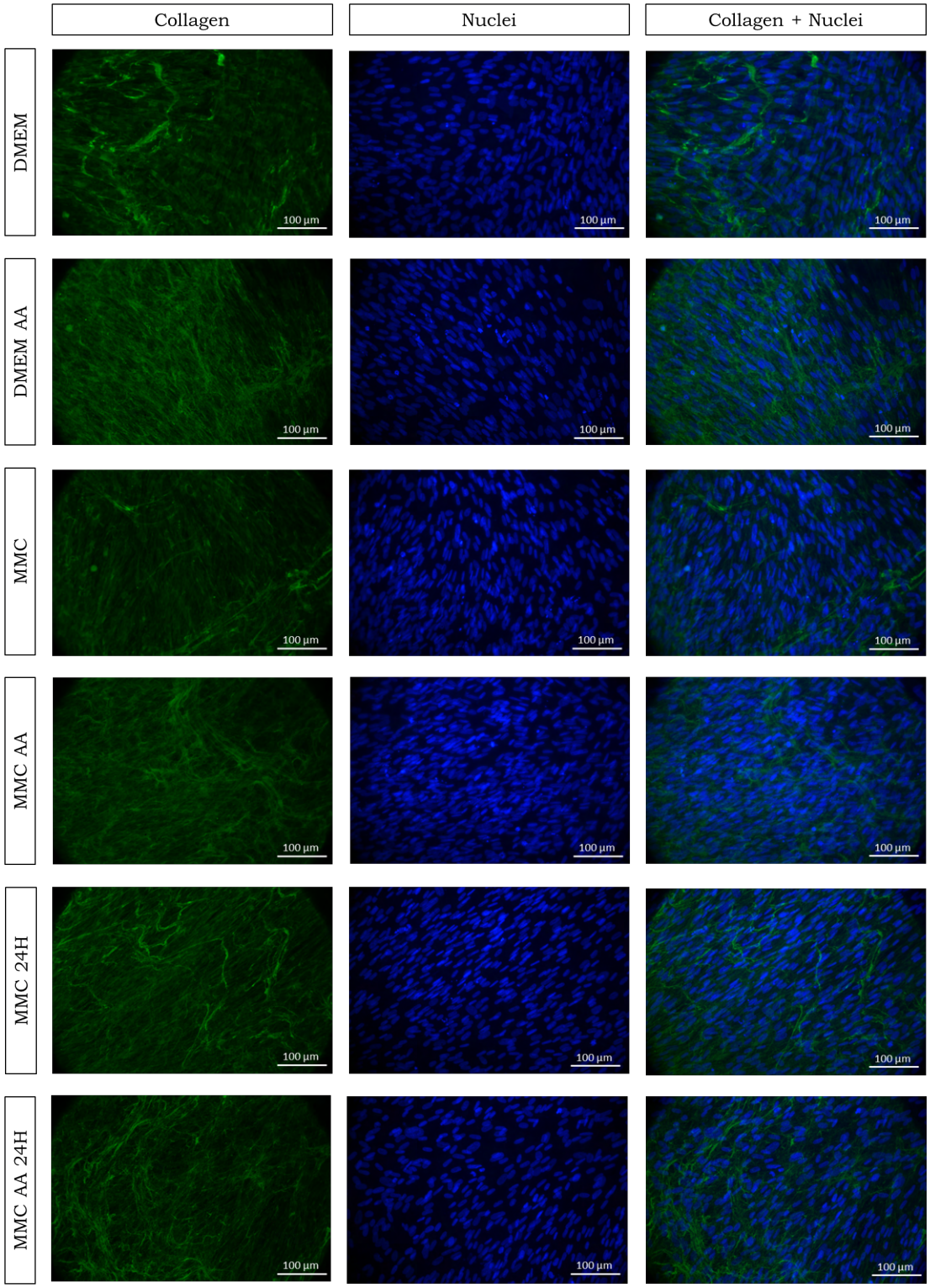

Figure 5.3: Immunocytochemistry images of collagen deposition in crowder optimization studies. Collagen and nuclei images were obtained with an exposure time of 1/2 seconds and 1/4 seconds, respectively. In the last column, composite images of collagen and nuclei staining are displayed. All the images were obtained with a 40x objective.

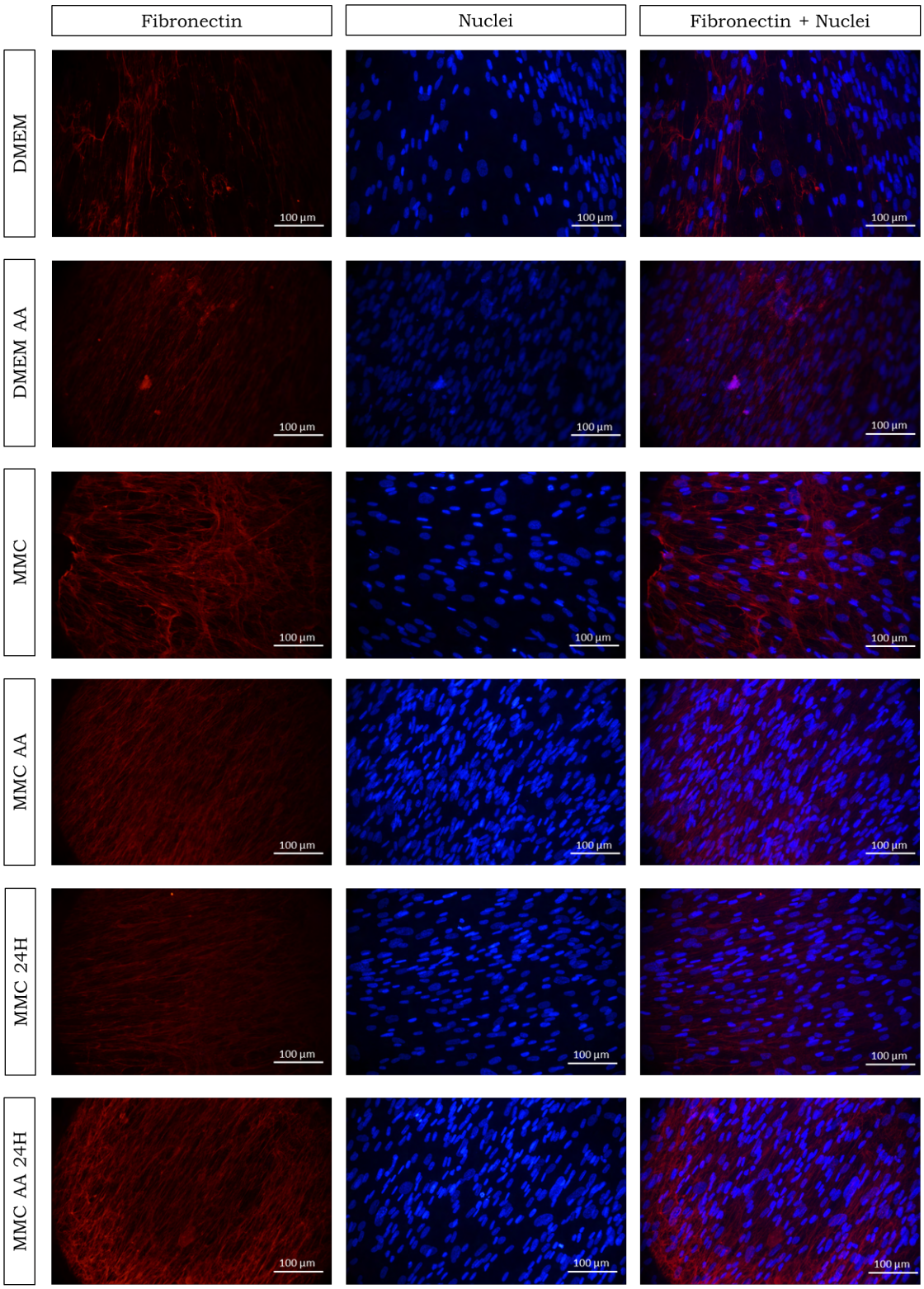

Figure 5.4: Immunocytochemistry images of fibronectin deposition in crowder optimization studies. Fibronectin and nuclei images were obtained with an exposure time of 1 second and 1/4 seconds, respectively. In the last column, composite images of fibronectin and nuclei staining are displayed. All the images were obtained with a 40x objective.

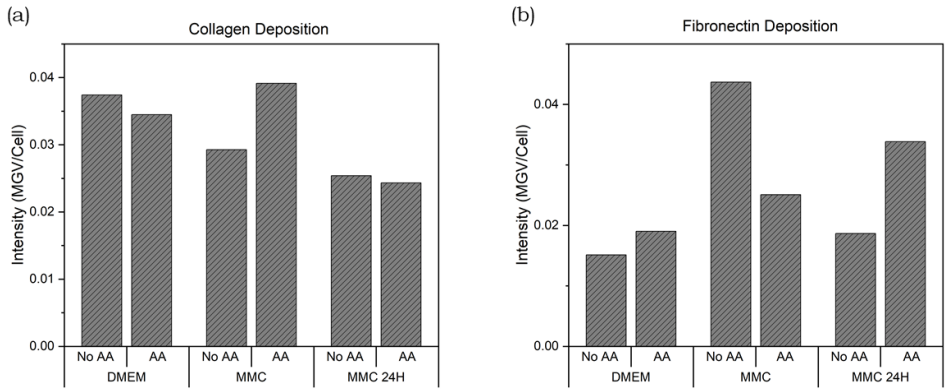

Figure 5.5: Deposition of ECM proteins in crowder optimization studies. Uncertainties are not provided since only one sample of each condition was analysed. (a) Collagen deposition (MGV/cell of images in figure 5.3). (b) Fibronectin deposition (MGV/cell of images in figure 5.4).

GTA is at the origin of the high autofluorescence problem. Genipin or N-ethyl-N'-(3-(dimethylamino)propyl)carbodiimide/N-hydroxysuccinimide (EDC/NHS) are crosslinking agents to take in consideration for further assessment. Dehydrothermal (DHT) treatment should not be considered as a crosslinking method for the dermal scaffolds since it requires matrix exposure to temperatures above 100 ºC, which is impracticable since PCL has a melting point at around 60 ºC. Considering these adversities, the remaining work was performed only with PCL matrices, which present almost no autofluorescence and allow good ECM visualization.

5.4 Analysis of Fibroblast Viability

The focus of this work is now the study of MMC on PCL matrices. However, beyond assessing ECM deposition, it is mandatory to understand if the metabolic activity and viability of fibroblasts is affected by the presence of MMC and in association with PCL scaffolds. For that, six different conditions were studied: to each supporting material condition, PCL or coverslips, three different culture media were used: without MMC, with PVP or with Fc.

Figure 5.7 shows the results of the resazurin assays performed. Through the analysis of the graph, it is relevant to highlight several points. Firstly, cellular viability significantly increases ($p < 0.05$) from the third day to fifth day in every condition, which indicates good cell proliferation along these days. However, from the fifth day to the seventh day, cellular viability slightly decreases in almost every condition, with the exception of cells cultured in PCL matrices crowded with PVP. These differences, with the exception of the condition PCL + Fc ($p < 0.05$), are not statistically significant ($p > 0.05$). The reduced variation in fibroblast viability from the fifth day to the seventh could indicate that cells reached a metabolic plateau. This could be associated to the fast fibroblast

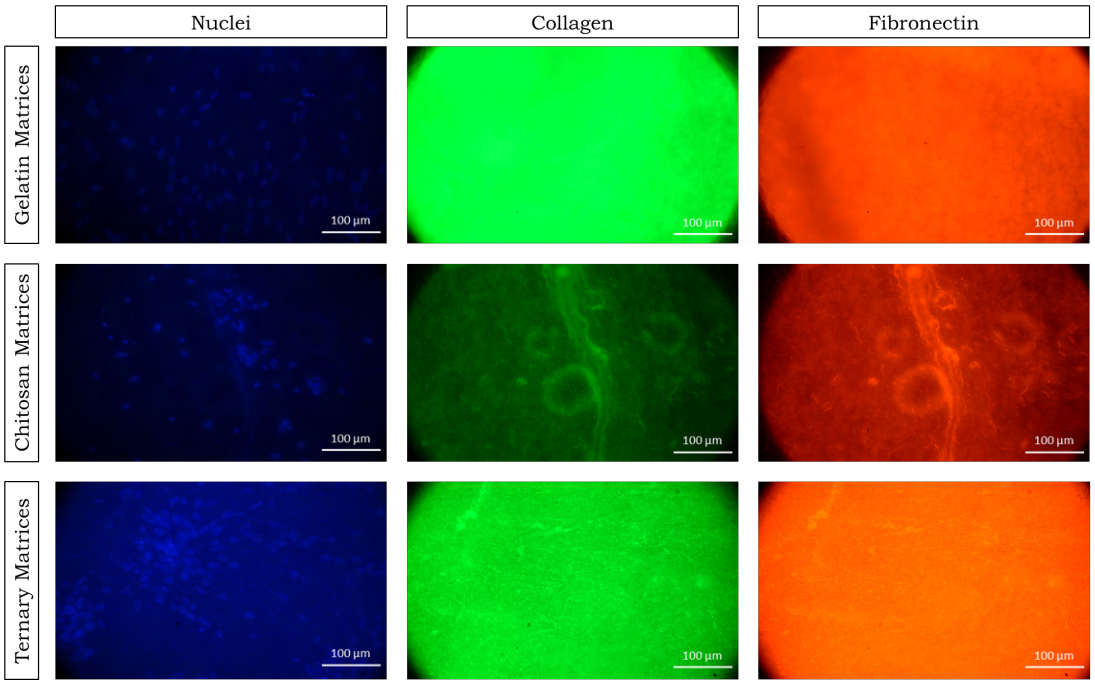

Figure 5.6: Immunocytochemistry images of GEL, CS and ternary matrices. For each matrix, a image of the blue, green and red channel is provided, where the staining of, respectively, nuclei, collagen and fibronectin, was performed. The visualization of collagen and fibronectin is impossible due to the autofluorescence of the matrices.

proliferation, resulting in confluence at around the fifth day, with posterior reduction in cellular metabolic activity. Considering that cells were seeded at a high density (25000 cells/cm^2), this hypothesis is even more likely.

Another important point to stress is that the determining factor of lower cellular viability is the use of PCL instead of coverslips. PCL conditions significantly decreased ($p < 0.05$) cellular viability in every crowding condition, at any time point, in comparison to the respective coverslip equivalent, with the exception of PVP supplementation at the seventh day, which significantly increased ($p < 0.05$). Previous studies with these matrices showed that cells seeded on PCL scaffolds present a cellular viability of 50% on the second day of culture in comparison to cells seeded on glass coverslips, due to low cell adhesion [73]. The authors suggest that the hydrophobic nature of the polymer and the few surface sites available for cellular interactions could be associated with the reduced adhesion. In our results, the lowest percentage of cellular viability at the third day in PCL matrices in comparison with control coverslips is 61%, which is achieved under DMEM supplementation. In the case of Fc and PVP supplementation, this value increases to 72% and 76%, respectively. Considering this, although our data is obtained at the third day (in [73], cell adhesion is measured at the second day), the cell adhesion in this work appeared to be above the expected. The authors suggest that, along the days, the proliferation rate of cells in PCL matrices matches the proliferation rate of cells in glass surface, which is also verified in our work. Therefore, the lower cellular viability in

PCL matrices is mostly due to the low cellular adhesion.

With these considerations being made, one should now focus on assessing if MMC had any impact on cell viability. PVP supplementation in coverslips at the third, fifth and seventh day time-points significantly decreased ($p < 0.05$) fibroblast viability in comparison to no MMC supplementation, which indicates that PVP implementation may directly affect the metabolic activity of these cells in coverslips. To our knowledge, only Rashid *et al.* [38] performed MMC-related studies with PVP. In this report, PVP 40 kDa at 18 % FVO (the most similar PVP condition to the one utilized in this dissertation) significantly increased the proliferation rate of fibroblasts seeded directly at the bottom of 24-well plate wells, which is indicative of high cellular viability. Rashid *et al.* [38] also suggest that viscosity could play an important role in cellular viability, as it is necessary that crowding solutions possess a viscosity level between the physiological range. No viscosity tests were performed with the PVP used in this work, so, to assess the possibility of viscosity being at the origin of this reduced viability, further tests should be performed, especially considering that PVP 55 kDa was never reported in the literature as a crowder.

Regarding the effect of PVP supplementation on cells seeded on PCL matrices, the results show that PVP significantly increased ($p < 0.05$) cellular viability at the 7 day time-point. However, in the remaining time-points, no significant differences ($p > 0.05$) are visualized in comparison to the uncrowded media. This difference at the seventh day is related to the fact that, unlike all the other conditions, cells in PCL matrices with PVP did not reach a plateau of proliferation between the fifth and seventh day (despite presenting similar cellular viability to the other groups in the previous time-points), remaining mitotically active and possibly proliferating until the seventh day. This indicates that PVP could have a distinct impact on cellular viability depending on the supporting material. However, further studies should be performed to assess this possibility.

Fc supplementation in coverslips significantly reduced ($p < 0.05$) fibroblast viability at the 7-day time-point. At the other time-points, no significant differences ($p > 0.05$) were visualized in comparison to uncrowded conditions. This suggests that, unlike PVP, Fc does not negatively impact cellular viability in coverslips, performing similarly to uncrowded conditions in the initial days. This meets what is widely mentioned in literature, as Fc does not appear to interfere significantly with cellular viability in comparison with typical culture medium. Although Fc decreases cellular viability at the seventh day, it still significantly allowed higher ($p < 0.05$) cellular viability in comparison with PVP. These results suggest that Fc may outperform PVP regarding fibroblast viability in glass coverslips.

Fc supplementation in PCL matrices significantly increased ($p < 0.05$) fibroblast viability at both 3 days and 5 days time-points. At the seventh day, no significant differences ($p > 0.05$) were obtained in comparison to the uncrowded group. Once again, there is a different effect of crowding supplementation on cellular viability depending on the supporting material. Alike PVP, Fc also increases the viability of fibroblasts cultured in PCL matrices in comparison to non-MMC groups. Literature findings are quite unclear about

the effect of MMC in cellular viability in 3D environments. On the one hand, Cámara-Torres *et al.* [61] showed that Fc maintained human mesenchymal stromal cells viability in 3D additive manufactured scaffolds. Additionally, Tsiapalis *et al.* [62] reported that CR did not significantly affect tenocyte viability in Biosyn™ scaffolds. On the other hand, Chen *et al.* [60] showed that Fc supplementation significantly decreased porcine chondrocytes viability in 3D models of engineered cartilage, while not showing any detrimental effect in 2D environments. Our work points towards the direction of the former results, as MMC effect actually seems to allow the increase, or at least the maintenance, of cellular viability in 3D models (PCL matrices). However, additional studies should be performed to confirm these results.

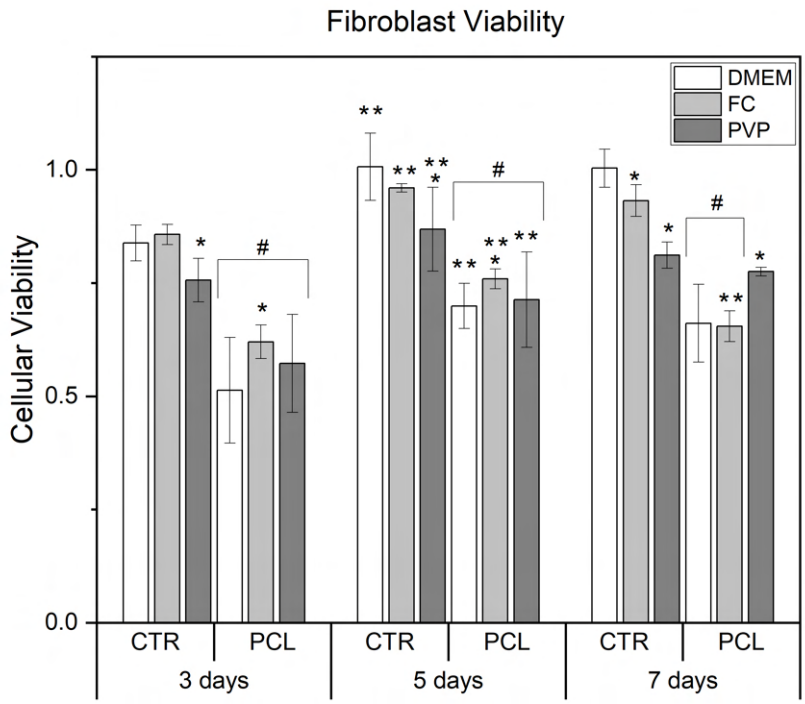

Figure 5.7: HFFF2 cell viability in the different crowding and supporting material conditions, at 3, 5 and 7 day time-point. The graph bars represent the cellular viability and respective uncertainty for each condition, which had at least three replicates. Statistically significant differences (p-value < 0.05) are represented by *, ** and #, where * is associated to a significant difference of the crowding condition to the control group (DMEM), in the same material and at the same time point; ** is associated to a significant difference to the previous time-point of the condition; # is associated to significant differences between materials (coverslip and PCL) at the same crowding condition and same time point.

5.5 Evaluation of ECM Deposition with Immunocytochemistry

This section assesses the results regarding ECM deposition in PCL with the different crowding conditions, which is the main objective of this work. Firstly, the immunocytochemistry images are analysed through direct observation. Then, average intensity measurements are provided in order to quantify protein deposition in the various conditions.

5.5.1 Image Analysis

Collagen type I and fibronectin deposition images are displayed, respectively, in figure 5.8 and figure 5.9. These are examples selected from a wide set of images for each condition which attempt to represent the typical deposition in the given condition. By analysing these images, the first thing that is noted is the increase in the number of nuclei along the days in every condition, which is partially consistent with the results obtained in 5.4. Although DAPI staining shows a typically greater number of cells at day 7, the highest cell population is achieved at day 5. This difference may be explained by the fact that cells present at day 7 are not as metabolically active as they were at day 5 and, thus, do not process resazurin as quickly as metabolically active cells do. Considering this increasing number of cells along the time-points, it is obviously expected that ECM deposition also increases in accordance to that. This tendency is verified in both figures, with some exceptions, such as fibronectin staining in the presence of supplementation, both in matrices and coverslips. Therefore, to compare the effect of MMC in images with different cell densities, normalization to the number of nuclei counted was performed.

Moreover, it is relevant to also point out differences in cell density and respective ECM distribution in PCL matrices, in comparison with glass coverslips. Cells are more equally distributed along the whole surface of coverslips, while in PCL matrices the cells seem to present cluster patterns, being localized in specific regions of the scaffold. This is related to the low cellular adhesion in these matrices, and is in accordance with previous studies [73], where PCL matrices showed a reduced coverage area by cells (less than 50% on the fourth culture day).

Additionally, some images regarding PCL matrices may present some blurriness. This may be due to the fact that cells migrated within the pores to a more interior region of the matrix. Therefore, by focusing the objective in more superficial cells, cells more incorporated inside the matrix may still be observed, but present blurriness. Although PCL scaffolds present high porosity (at around 80%), the internalization of cells in the matrices is more dependent of the pore size. Since pores size of PCL scaffolds is relatively small, cells may have difficulty in migrating to more interior regions of the matrix, which explains why the majority of the cells are present in the more superficial layers of the PCL matrices. However, this behavior is not clear, as two previous studies report opposite observations. In [74], Vero cells did not adequately migrate into the interior of

the structure, while in [73] HFFF2 showed good incorporation into the matrix. In our work, we were able to identify adhered cells in several plans along the PCL matrix by using different focus, which seems to corroborate what was observed in the latter study, although no confocal microscopy images were obtained to confirm this. A justification for this difference could be related to the size of the cells, however, HFFF2 present a way bigger length in comparison to Vero cells, which would, in theory, result in a more difficult infiltration onto the matrix, which is not verified.

With this being said, the focus is now to understand how the production of the proteins studied was affected by the different conditions at the same time-point. An interesting occurrence verified both in collagen and fibronectin deposition images, and both in coverslips and PCL matrices, is that Fc seemed to enable a better ECM formation between more separated cells, in comparison to DMEM groups. Fc appeared to allow greater fiber elongation, forming sequences of ECM-interconnected cells, while in groups without MMC, ECM deposition appeared to be more localized within the proximity of each cell. This is specially verified at the third day time-point, as the lower number of cells allows an easier assessment, however, in the subsequent days this can also be observed. These observations are consistent with what is found in the literature, as Fc seems to promote higher collagen type I and fibronectin deposition. However, several reports in literature mention that Fc even allows a 5-fold increase in ECM deposition in comparison to uncrowded groups [38], [52], [64], which clearly does not occur in our work, being confirmed by intensity quantification further analysed (figure 5.10). Actually, by comparing our images with the ones in figure 3.2, these differences are quite evident. Nonetheless, in conditions with PCL matrices, which to our knowledge no MMC studies have been performed with, Fc also seems to outperform no-MMC groups, showing a similar behavior to what is observed in glass coverslips.

In regard to images with PVP crowding, one should note that some images may show some blurriness, which could affect to a certain degree image perception. By visualizing the images for both fibronectin and collagen, the behavior of deposition of these proteins is less clear than what was verified with Fc. In coverslips, collagen deposition under PVP appears to be increased and also show an easier ECM interconnection between cells, when in comparison with MMC untreated groups. However, in PCL matrices, it is quite hard to understand collagen deposition behavior, especially in day 5 and day 7. Regarding fibronectin images, cells in coverslips supplemented with PVP appear to have increased fibronectin deposition. Even though these images have an exposure time superior to the remaining images, which necessarily increases average intensity and difficults comparison, it seems that an increase in fibronectin deposition was verified, at least in comparison with groups without MMC. When it comes to PCL matrices, again, the behavior is quite unclear.

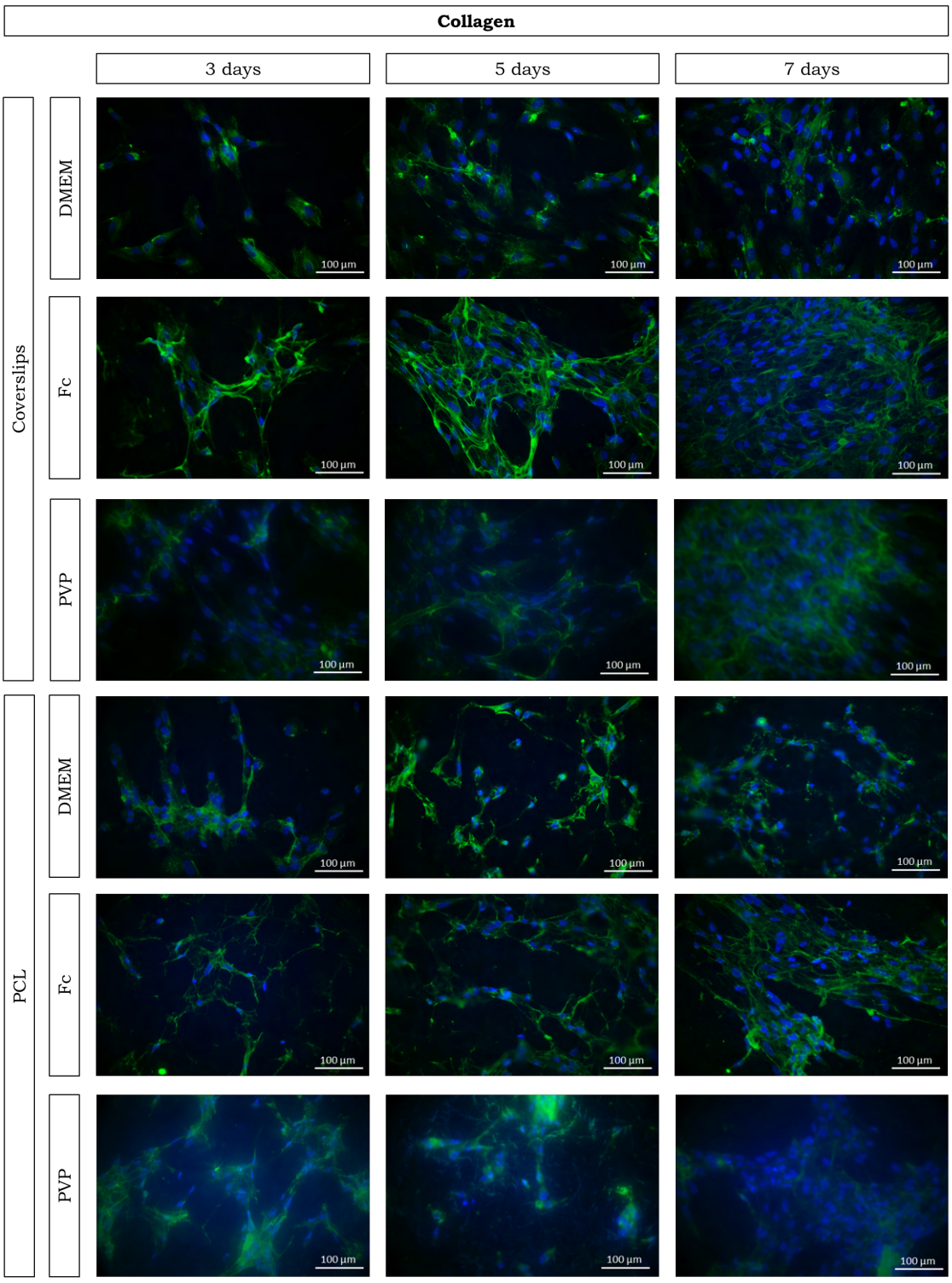

Figure 5.8: Immunocytochemistry images of collagen deposition in the different crowding and supporting material conditions, at 3, 5 and 7 day time-point. These images were obtained by overlaying collagen staining images with nuclei staining images. All the images were obtained with a 40x objective. Green channel images (collagen) had an exposure time of 1/2 seconds, while blue channel images (nuclei) had an exposure time of 1/4 seconds.

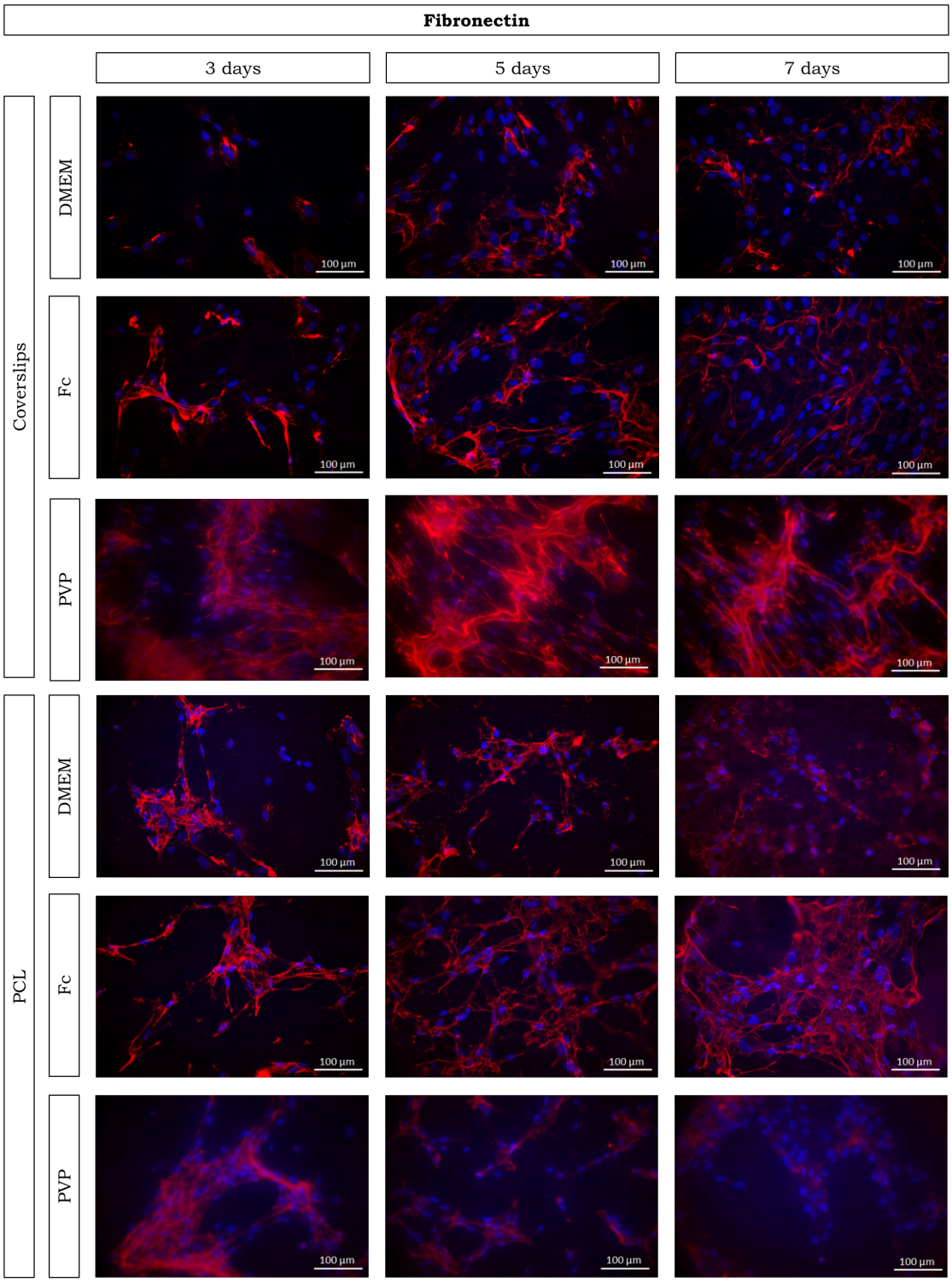

Figure 5.9: Immunocytochemistry images of fibronectin deposition in the different crowding and supporting material conditions, at 3, 5 and 7 day time-point. These images were obtained by overlaying fibronectin staining images with nuclei staining images. All the images were obtained with a 40x objective. Red channel images (fibronectin) had an exposure time of 1/6 seconds, except in PVP + coverslips conditions where it was 1/2 seconds (some difficulties were faced in assessing fibronectin deposition with the usual 1/6 seconds), while blue channel images (nuclei) had an exposure time of 1/4 seconds.

5.5.2 Intensity Quantification

To complement direct image observation, fibronectin and collagen deposition were quantified through intensity measurements of several images, as described earlier in section 4.4.4. The results are presented in figure 5.10.

Starting by analysing the graph referent to collagen deposition, statistical tests show that PVP supplementation in glass coverslips significantly reduced ($p < 0.05$) collagen deposition in comparison to DMEM supplementation at all-time points. Comparing these outcomes with cellular viability results, it is possible to associate a lower cellular viability, which was verified at all time-points in glass coverslips with PVP, with lower ECM deposition. Actually, collagen type I is the key structural constituent of the ECM of fibroblasts, and a reduced production of this protein impairs ECM formation and, ultimately, impairs proper cell proliferation. Rashid *et al.* [38] reports that PVP 40 kDa at 18% FVO significantly increased ($p < 0.01$) collagen type I deposition by human dermal fibroblasts (in glass surface) in comparison to non-MMC groups. The authors suggest that this increase was due to moderate levels of polydispersity of PVP 40 kDa (polydispersity index = 0.304, measured via dynamic light scattering), as high polydispersity is associated with a greater ECM deposition, as already explained. Actually, PVP 40 kDa has a higher polydispersity index than Fc 70 kDa and Fc 400 kDa (0.224 and 0.240, respectively), which is indicative of the potential of PVP as a macromolecular crowder. Our work, although using PVP 55 kDa at the same FVO, is contradicting with these findings. This could be due to the fact that PVP 55 kDa has a more reduced polydispersity index than what would be expected considering the polydispersity index of a PVP with a relatively similar molecular weight (40 kDa), however, it is not possible to confirm this since it was not measured along the work nor was found in literature. Another possible cause is viscosity, which was also not assessed, as high viscosity is known to decrease the diffusion rate and the kinetics of reactions controlled by this transport method, which is the case of procollagen conversion to collagen, and collagen deposition. Rashid *et al.* [38] defends that matrix deposition depends on the tradeoff between EVE and viscosity, enhancing the importance of studying crowders viscosity, which should be performed in the continuation of this work.

Considering fibronectin deposition, the outcomes are quite different to what was achieved with collagen deposition. The results showed that PVP significantly increased ($p < 0.05$) fibronectin deposition at the 5 day time-point, while in the remaining time-points no statistically significant differences were achieved, in comparison to the uncrowded group. It is important to stress that it is not possible to perform intensity comparisons between collagen type I and fibronectin deposition at the same conditions, due to the influence of several factors in image intensity, namely: the usage of different primary antibody concentrations, the efficiency of antigen-antibody binding, the usage of different secondary antibodies, the possibility of variations in the number of fluorophores coupled to each secondary antibody, or differences in the process of excitation, emission and detection of radiation. Therefore, these comparisons must only be performed by assessing

differences observed in each staining to a certain control group in the same staining. Considering this, PVP could influence differently the deposition of collagen type I and fibronectin, since in the former the deposition is clearly impaired in all time points, while in the latter PVP actually allowed greater deposition in one of the time-points (in comparison to respective uncrowded groups). However, considering that PVP + coverslip images were obtained with a higher exposure time, even though that image normalization was performed by background subtraction, this correction is not enough for adequate comparison. Therefore, the higher MGV of these images is most definitely due to this difference in the exposure time. Nonetheless, theoretical hypothesis for this difference should also be considered. Rashid *et al.* [38] reports that PVP 40 kDa allows greatest collagen type I deposition at a FVO of 18%, which is the used FVO in our work, however, concerning fibronectin deposition, the greatest deposition is achieved at a FVO of 36%, which is indicative of the different impact of MMC in each protein deposition. However, this is quite the opposite of what is verified in our work, which leaves the idea that PVP 55 kDa may have a distinct optimal FVO percentage for each protein deposition, in comparison to PVP 40 kDa. These results could make our assumption that PVP 55 kDa has a similar impact to PVP 40 kDa at the same FVO fall apart. Therefore, for further work, physico-chemical properties which could influence the efficiency of PVP 55 kDa as a crowder like polydispersity index, hydrodynamic radius or viscosity should be assessed to come close to an explanation for these results, or make use of other, more well tested, PVP molecular weights like PVP 40 kDa or PVP 360 kDa.

Nonetheless, it is still important to assess how PVP 55 kDa crowding performed in regard to PCL matrices. The results show that no significant differences ($p > 0.05$) were achieved in PCL + PVP conditions, at any time point, in comparison to PCL + DMEM conditions, both for collagen type I and fibronectin deposition, not seeming to have a determinant impact in ECM formation. Actually, in PCL matrices PVP did not significantly decrease collagen type I deposition, as verified in coverslips, not presenting significant differences to the control group. As already stated, Chen *et al.* [60] reports that MMC decreases ECM deposition in 3D environments, despite increasing it in 2D environments (see section 3.1.9 for more details). However, Tsiapalis *et al.* [62] and Cámara-Torres *et al.* [61] showed that ECM deposition was increased in 3D models in the presence of MMC. Our studies partially support the latter findings, suggesting that PVP 55 kDa seems to, at least, not impair collagen type I deposition in 3D environments. Oddly, in 2D environments it substantially decreased collagen type I deposition.

When it comes to Fc supplementation, it significantly increased ($p < 0.05$) both collagen type I and fibronectin deposition in glass coverslips at third day post-seeding, in comparison to the respective non-MMC groups of each protein. However, in the remaining time-points, no significant differences ($p > 0.05$) were observed for both proteins. As already mentioned in chapter 3, Fc 70/400 cocktail is widely mentioned in literature as being able to consistently increase the deposition of several ECM proteins. However, in our work, it seems that this potential is quite inhibited after surpassing the third day of

culture. Additionally, as mentioned earlier, in our work Fc supplementation does not allow substantial fold increases of collagen type I or fibronectin deposition in comparison to control groups, as is often stated in literature. In here, only Fc supplementation in coverslips at the third day came close to a two-fold increase, although still not achieving it, suggesting a clear under-performance of the crowder. Nonetheless, it would be interesting to assess what could provoke this difference in ECM deposition per cell between time-points. We suggest that this is because Fc utilization, and general MMC utilization, has the greatest impact in the initial days of culture. In here, the extracellular medium is extremely uncrowded, as cells are still yet to proliferate and intense ECM deposition to occur. Therefore, Fc plays an important role in allowing EVE, and ultimately stimulating greater ECM deposition in the initial days. However, as the culture advances, even uncrowded conditions begin to achieve a decent ECM deposition and cell proliferation. Thus, from the moment there has been achieved a decent amount of ECM deposition and cell proliferation in these, the impact of MMC is not as crucial as in the initial stages, where there were no ECM proteins present, which also inherently contribute to the MMC effect. Therefore, at later stages, MMC and non-MMC groups may present similar ECM deposition, however, in the initial days, MMC groups enable a more immediate and enhanced ECM deposition. This explains why, during image analysis, the increase of collagen type I and fibronectin deposition was more clear in images at the third day.

Regarding PCL matrices, Fc supplementation only significantly increased ($p < 0.05$) collagen type I deposition at the third day time point, in comparison to uncrowded groups. In the remaining time-points, and in fibronectin deposition, no significant differences ($p > 0.05$) were observed. Unlike PVP, Fc still behaves accordingly in PCL matrices to what is verified in coverslips, as it seems to also increase deposition of both proteins at, in least, one time-point (in comparison to DMEM groups in the same material). This could indicate that, although PCL matrices inherently diminish ECM deposition, Fc supplementation could be beneficial in PCL matrices, as it allowed similar or greater ECM deposition than DMEM groups.

It is also interesting to assess how using PCL matrices affects ECM deposition in the same crowding condition, in comparison with glass coverslips. Collagen type I deposition under Fc supplementation was significantly decreased ($p < 0.05$) using PCL matrices, in comparison to glass coverslips with the same crowding condition, at all time points. At the third day, collagen type I deposition without MMC supplementation was also significantly decreased ($p < 0.05$) in PCL matrices. Considering fibronectin deposition, it was significantly decreased ($p < 0.05$) for both Fc supplementation at third day and PVP supplementation at the seventh day, in PCL matrices. There is a clear tendency for the diminishing of ECM deposition in PCL matrices, relatively to glass coverslips, in all crowding conditions, as it would be expected considering the lower cellular viability in PCL matrices.

Overall, our work indicates that Fc outperformed PVP, especially in collagen deposition. Fc crowding significantly increased ($p < 0.05$) collagen type I deposition in

coverslips at all time-points in comparison to PVP crowding, and in PCL at the third day. However, regarding fibronectin deposition, no significant differences ($p > 0.05$) were observed. In [38], Fc cocktail also had the greatest effect in enhancing collagen type I deposition, outperforming both PVP 40 kDa and PVP 360 kDa, however, the latter ones offer a good alternative to the former due to their lower cost and better viscosity properties along the various FVOs. In our work, PVP 55 kDa was actually detrimental for ECM production in most conditions, not constituting a solid alternative to Fc cocktail. But even Fc cocktail, although inducing significant ECM deposition (especially collagen type I) in some conditions, did not have as good outcomes as expected, such as the ones seen in [38], [52], [64], per example.

Finally, experimental flaws should also be considered as a possible cause for these results. First off, several different cultures were performed to achieve these results, studying each crowder separately. This was carried out as so because the required material associated to the high number of samples, and the high number of samples themselves, offered an important obstacle. Thus, it would be interesting to simultaneously assess all the conditions studied in just one culture, as a way to reduce variability between cultures, ensuring that the influence of crowders in cellular viability and ECM deposition is compared without the variability of cell culture. Secondly, in immunocytochemistry procedures, the amount of samples for each condition, as well as the amount of images acquired for each sample, may have been insufficient to provide more precise and significant results. The usage of confocal microscopy instead of fluorescence microscopy could also allow a better ECM visualization. Finally, one should consider that there are various steps involved in the process of ECM deposition quantification, such as immunocytochemistry, image acquisition, image treatment and the quantification process itself, which may offer some adversities. It would be interesting to carry out other quantification methods, or to repeat the experiment using the same culture to confirm the results obtained.

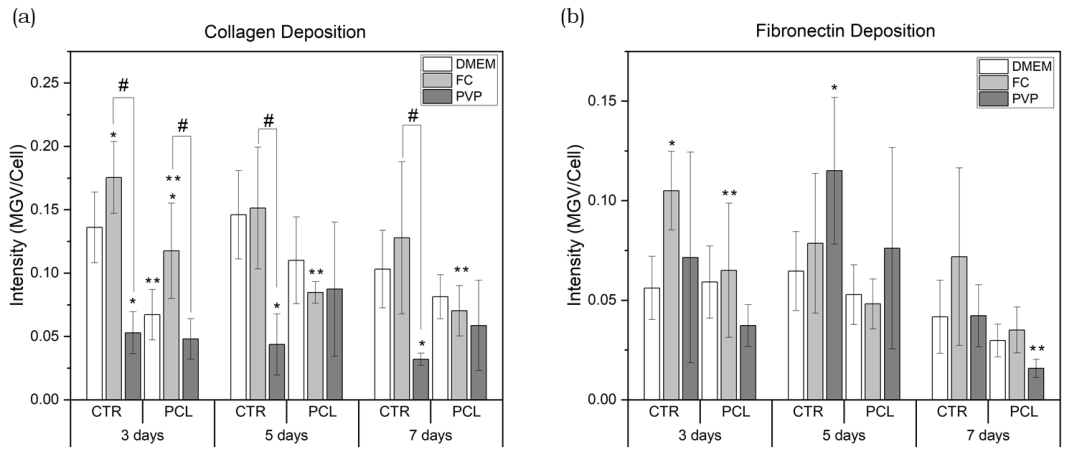

Figure 5.10: Deposition of ECM proteins, (a) collagen and (b) fibronectin, in the different supporting materials and crowding conditions at days 3, 5 and 7. The bars represent average intensity for each condition, at each time-point, obtained from, at least, two images in different points of a minimum of two samples. Statistically significant differences (p-value < 0.05) are represented by *, ** and #, where * is associated to a significant difference of the crowding condition to the control group (DMEM), in the same material and at the same time point; ** is associated to significant differences between materials (coverslip and PCL) at the same crowding condition and same time point; # is associated so significant differences between Fc and PVP in the same material and at the same time-point

6

Conclusion and Future Perspectives

This work intended to assess if the MMC effect could enhance the metabolic and regenerative ability of dermal fibroblasts, seeded on the dermal scaffold studied in the ambit of the iSkin2 project. For this, cellular viability via resazurin assays and ECM deposition visualization and quantification via immunocytochemistry procedures were performed, in the presence of two crowding conditions: Fc cocktail and PVP 55 kDa.

Before this could be achieved, several optimization studies were performed regarding both crowding conditions and the immunocytochemistry procedure. In the former, we concluded that MMC should be implemented right at cell seeding and that AA supplementation should not be performed. In the latter, we concluded which antibodies allowed a better visualization of collagen and fibronectin, and achieved an optimized protocol.

In this study, we showed that the autofluorescence of the dermal scaffold represents a major impediment for an adequate visualization of immunocytochemistry images. Accordingly, these studies were performed using PCL scaffolds, which do not present autofluorescence.

Resazurin assays showed that Fc cocktail did not significantly impair cellular viability in most conditions, while actually allowing better cellular viability than non-MMC groups in the scaffold studied. PVP 55 kDa reduced cellular viability in 2D environments, however, in fibroblasts seeded in PCL matrices, it did not impair, or even increased cellular viability. We conclude that Fc supplementation was the best option for fibroblast viability in PCL matrices.

Moreover, this work showed that Fc supplementation had greater influence in enhancing ECM deposition in the early culture days, especially collagen type I, including in PCL matrices. PVP 55 kDa supplementation actually decreased ECM deposition in most conditions, although in PCL matrices this decrease was less significant. By image analysis, MMC supplementation appeared to allow greater deposition of both proteins, although sometimes contradictory to what is verified in ECM deposition quantification. We still believe that MMC real potential was not evident with these results, as literature shows greater increase in ECM deposition, especially with Fc cocktail. We propose the realization of other complementary methods, such as real-time quantitative polymerase chain

reaction (RT-qPCR), to assess genetic expressions for ECM production, as the results obtained might have been influenced by difficulties related to the immunocytochemistry procedure.

The first proposed objective was achieved, as the dermal scaffolds were produced during this work. However, the studies performed showed that it was not viable to continue the work with these matrices due to autofluorescence, therefore, the remaining points were achieved using PCL matrices: analysis of fibroblast viability in PCL matrices in the presence of the crowders, and analysis of ECM deposition by fibroblast in PCL matrices in the presence of the crowders. Conducting these studies in PCL matrices not only allowed to better understand the MMC effect in 3D environments, but also provided an initial idea about the performance of the dermal scaffold in these conditions, as it is also composed by PCL. This way, this study contributed to a better understanding about the MMC effect, and presented advances in regard to the iSkin2 project.

Overall, this work showed that the use of Fc cocktail as a macromolecular crowder, although not reaching the results seen in literature, outperformed the use of PVP 55 kDa, offering an interesting alternative to the uncrowded cell medium. Additionally, we showed promising results regarding the MMC effect in 3D environments, namely PCL matrices, as crowders actually seem to have improved, or at least not impaired, cellular viability and collagen type I deposition in these matrices.

For further investigation, the following suggestions are made: First, since the autofluorescence of dermal scaffolds conditioned the realization of immunocytochemistry studies in these matrices, and considering that the use of GTA as a crosslinking agent could be at the origin of this problem, other crosslinking agents such as EDC/NHS or genipin should be tested. Secondly, physico-chemical properties of PVP 55 kDa such as polydispersity index and solution viscosity should be assessed, in order to better understand its potential as a macromolecular crowder. Additionally, other macromolecular crowders described in the literature, such as CR, DxS or PVPs with different MW (40 kDa or 360 kDa) could be assessed. Moreover, alternative methods for the quantification of ECM deposition or production should be considered, since through immunocytochemistry it may be quite challenging to obtain accurate quantifications. Accordingly, RT-qPCR procedures are scheduled to be performed to assess the genetic expression of collagen type I and fibronectin, indicating if the production of these proteins is altered in the presence of the MMC effect, and in PCL matrices. Finally, since the studies performed for each crowder were conducted in separated cultures, it would be interesting to perform them in the same culture, although it may be quite challenging because of the high number of samples, and all the material required.

We finish by paraphrasing Tsiapalis *et al.* [28], saying that it is impossible to expect a physiological behavior of cells *in vitro* when we drown them in such a dilute and macromolecule-deprived sea of medium. Like them, we believe that MMC is an important component of TE's future.

Bibliography

[1] J. M. Lourenço, *The NOVAthesis LaTeX Template User's Manual*, NOVA University Lisbon, 2021. [Online]. Available: https://github.com/joaomlourenco/novathesis/raw/master/template.pdf.

[2] R. Langer and J. Vacanti, "Tissue Engineering", *Science*, vol. 260, no. 5110, pp. 920–926, 1993, ISSN: 19388098. DOI: 10.1080/00131725009342110.

[3] A. Hasan, "Tissue Engineering for Artificial Organs", *Tissue Engineering for Artificial Organs: Regenerative Medicine, Smart Diagnostics and Personalized Medicine*, vol. 1-2, pp. 1–34, 2017. [Online]. Available: http://doi.wiley.com/10.1002/9783527689934.

[4] X. Ren, M. Zhao, B. Lash, M. M. Martino, and Z. Julier, "Growth Factor Engineering Strategies for Regenerative Medicine Applications", *Frontiers in Bioengineering and Biotechnology*, vol. 7, no. 469, pp. 1–9, 2020, ISSN: 22964185. DOI: 10.3389/fbioe.2019.00469.

[5] C. S. Ribeiro, F. Leal, and T. Jeunon, "Skin anatomy, histology, and physiology", in *Daily Routine in Cosmetic Dermatology*, M. Issa and B. Tamura, Eds., Springer, 2016, ch. 1, pp. 1–12.

[6] P. Kolarsick, M. Kolarsick, and C. Goodwin, "Anatomy and physiology of the skin.", *Journal of the Dermatology Nurses' Association*, vol. 3, p. 366, 2011. DOI: doi:10.1097/JDN.0b013e31823cccbe.

[7] J. R. Yu, J. Navarro, J. C. Coburn, *et al.*, "Current and Future Perspectives on Skin Tissue Engineering: Key Features of Biomedical Research, Translational Assessment, and Clinical Application", *Advanced Healthcare Materials*, vol. 8, no. 5, pp. 1–19, 2019, ISSN: 21922659. DOI: 10.1002/adhm.201801471.

[8] C. Singh, "Skin anatomy and physiology", in *Wound Care Made Incredibly Visual!*, 2018, pp. 1–10, ISBN: 9781496398277. DOI: 10.5005/jp/books/12699_2.

[9] P. Bainbridge, "Wound healing and the role of fibroblasts", *Journal of Wound Care*, vol. 22, no. 8, pp. 407–412, 2013, ISSN: 09690700. DOI: 10.12968/jowc.2013.22.8.407.

[10] A. M. Wojtowicz, S. Oliveira, M. W. Carlson, A. Zawadzka, C. F. Rousseau, and D. Baksh, "The importance of both fibroblasts and keratinocytes in a bilayered living cellular construct used in wound healing", *Wound repair and regeneration : official publication of the Wound Healing Society [and] the European Tissue Repair Society*, vol. 22, no. 2, pp. 246–255, 2014, ISSN: 1524475X. DOI: 10.1111/wrr.12154.

[11] W. P. Daley, S. B. Peters, and M. Larsen, "Extracellular matrix dynamics in development and regenerative medicine", *Journal of Cell Science*, vol. 121, no. 3, pp. 255–264, 2008, ISSN: 00219533. DOI: 10.1242/jcs.006064.

[12] H. Järveläinen, A. Sainio, M. Koulu, T. N. Wight, and R. Penttinen, "Extracellular matrix molecules: Potential targets in pharmacotherapy", *Pharmacological Reviews*, vol. 61, no. 2, pp. 198–223, 2009, ISSN: 00316997. DOI: 10.1124/pr.109.001289.

[13] M. Raghunath and D. I. Zeugolis, "Transforming eukaryotic cell culture with macromolecular crowding", *Trends in Biochemical Sciences*, vol. 46, no. 10, pp. 805–811, 2021, ISSN: 13624326. DOI: 10.1016/j.tibs.2021.04.006. [Online]. Available: https://doi.org/10.1016/j.tibs.2021.04.006.

[14] D. A. Carrino, P. Önnerfjord, J. D. Sandy, *et al.*, "Age-related changes in the proteoglycans of human skin. Specific cleavage of decorin to yield a major catabolic fragment in adult skin", *Journal of Biological Chemistry*, vol. 278, no. 19, pp. 17 566–17 572, 2003, ISSN: 00219258. DOI: 10.1074/jbc.M300124200.

[15] L. E. Tracy, R. A. Minasian, and E. J. Caterson, "Extracellular Matrix and Dermal Fibroblast Function in the Healing Wound", *Advances in Wound Care*, vol. 5, no. 3, pp. 119–136, 2016, ISSN: 21621934. DOI: 10.1089/wound.2014.0561.

[16] T. Z. Ling, A. Nather, and H. H. W. Dennis, "Basic science of wound healing", *The Diabetic Foot*, pp. 89–96, 2012. DOI: 10.1142/9789814417013_0008.

[17] L. Cañedo-Dorantes and M. Cañedo-Ayala, "Skin acute wound healing: A comprehensive review", *International Journal of Inflammation*, vol. 2019, 2019, ISSN: 20420099. DOI: 10.1155/2019/3706315.

[18] S. Werner, T. Krieg, and H. Smola, "Keratinocyte-fibroblast interactions in wound healing", *Journal of Investigative Dermatology*, vol. 127, no. 5, pp. 998–1008, 2007, ISSN: 15231747. DOI: 10.1038/sj.jid.5700786.

[19] R. Ahmadi and J. D. De Bruijn, "Biocompatibility and gelation of chitosan-glycerol phosphate hydrogels", *Journal of Biomedical Materials Research - Part A*, vol. 86, no. 3, pp. 824–832, 2008, ISSN: 15493296. DOI: 10.1002/jbm.a.31676.

[20] K. Kojima, Y. Okamoto, K. Kojima, *et al.*, "Effects of chitin and chitosan on collagen synthesis in wound healing", *Journal of Veterinary Medical Science*, vol. 66, no. 12, pp. 1595–1598, 2004, ISSN: 09167250. DOI: 10.1292/jvms.66.1595.

[21] J. Venkatesan, S. K. Kim, and T. W. Wong, *Chitosan and Its Application as Tissue Engineering Scaffolds*. Elsevier Inc., 2015, pp. 133–147, ISBN: 9780323353038. DOI: 10.1016/B978-0-323-32889-0.00009-1.

[22] S. Samimi Gharaie, S. Habibi, and H. Nazockdast, "Fabrication and characterization of chitosan/gelatin/thermoplastic polyurethane blend nanofibers", *Journal of Textiles and Fibrous Materials*, vol. 1, pp. 1–8, 2018, ISSN: 2515-2211. DOI: 10.1177/2515221118769324.

[23] M. Nikkhah, M. Akbari, A. Memic, A. Dolatshahi-pirouz, and A. Khademhosseini, "Gelatin-based biomaterials for tissue engineering and stem cell bioengineering", in *Biomaterials from Nature for Advanced Devices and Therapies*, N. M. Neves and R. L. Reis, Eds., Wiley, 2016, ch. 3, pp. 37–62.

[24] N. Siddiqui, S. Asawa, B. Birru, R. Baadhe, and S. Rao, "PCL-Based Composite Scaffold Matrices for Tissue Engineering Applications", *Molecular Biotechnology*, vol. 60, no. 7, pp. 506–532, 2018, ISSN: 15590305. DOI: 10.1007/s12033-018-0084-5. [Online]. Available: https://doi.org/10.1007/s12033-018-0084-5.

[25] S. Agarwal, J. H. Wendorff, and A. Greiner, "Use of electrospinning technique for biomedical applications", *Polymer*, vol. 49, no. 26, pp. 5603–5621, 2008, ISSN: 00323861. DOI: 10.1016/j.polymer.2008.09.014. [Online]. Available: http://dx.doi.org/10.1016/j.polymer.2008.09.014.

[26] I. Jun, H. S. Han, J. R. Edwards, and H. Jeon, "Electrospun fibrous scaffolds for tissue engineering: Viewpoints on architecture and fabrication", *International Journal of Molecular Sciences*, vol. 19, no. 3, 2018, ISSN: 14220067. DOI: 10.3390/ijms19030745.

[27] R. J. Ellis and A. P. Minton, "Join the crowd", *Nature*, vol. 425, no. 6953, pp. 27–28, 2003, ISSN: 00280836. DOI: 10.1038/425027a.

[28] D. Tsiapalis and D. I. Zeugolis, "It is time to crowd your cell culture media – Physicochemical considerations with biological consequences", *Biomaterials*, vol. 275, no. May, p. 120 943, 2021, ISSN: 18785905. DOI: 10.1016/j.biomaterials.2021.120943. [Online]. Available: https://doi.org/10.1016/j.biomaterials.2021.120943.

[29] S. B. Zimmerman and A. P. Minton, "Macromolecular crowding: biochemical, biophysical, and physiological consequences", *Annu. Rev. Biophys. Biomol. Struct.*, vol. 22, pp. 27–65, 1993.

[30] I. M. Kuznetsova, K. K. Turoverov, and V. N. Uversky, "What macromolecular crowding can do to a protein", *International Journal of Molecular Sciences*, vol. 15, no. 12, pp. 23 090–23 140, 2014, ISSN: 1422-0067. DOI: 10.3390/ijms151223090. [Online]. Available: https://www.mdpi.com/1422-0067/15/12/23090.

[31] P. Benny, C. Badowski, E. B. Lane, and M. Raghunath, "Making more matrix: enhancing the deposition of dermal-epidermal junction components in vitro and accelerating organotypic skin culture development, using macromolecular crowding", *Tissue engineering. Part A*, vol. 21, no. 1-2, pp. 183–192, 2015, ISSN: 1937335X. DOI: 10.1089/ten.TEA.2013.0784.

[32] C. Chen, F. Loe, A. Blocki, Y. Peng, and M. Raghunath, "Applying macromolecular crowding to enhance extracellular matrix deposition and its remodeling in vitro for tissue engineering and cell-based therapies", *Advanced Drug Delivery Reviews*, vol. 63, no. 4, pp. 277–290, 2011, ISSN: 0169409X. DOI: 10.1016/j.addr.2011.03.003. [Online]. Available: http://dx.doi.org/10.1016/j.addr.2011.03.003.

[33] G. J. Laurent, "Rates of collagen synthesis in lung, skin and muscle obtained in vivo by a simplified method using [3H]proline", *Biochemical Journal*, vol. 206, no. 3, pp. 535–544, 1982, ISSN: 02646021. DOI: 10.1042/bj2060535.

[34] B. Goldberg, "Kinetics of processing of type I and type III procollagens in fibroblast cultures", *Proc. Natl. Acad. Sci. U. S. A.*, vol. 74, no. 8, pp. 3322–3325, 1977.

[35] Merck. "Ficoll® 400 for gradient centrifugation". (2022), [Online]. Available: https://www.sigmaaldrich.com/PT/en/technical-documents/protocol/cell-culture-and-cell-culture-analysis/primary-cell-culture/ficoll-400 (visited on 02/03/2022).

[36] ——, "Dextran sulfate". (2022), [Online]. Available: https://www.sigmaaldrich.com/PT/en/technical-documents/protocol/protein-biology/protein-pulldown/dextran-sulfate (visited on 02/03/2022).

[37] M. Teodorescu and M. Bercea, "Poly(vinylpyrrolidone) – A Versatile Polymer for Biomedical and Beyond Medical Applications", *Polymer - Plastics Technology and Engineering*, vol. 54, no. 9, pp. 923–943, 2015, ISSN: 15256111. DOI: 10.1080/03602559.2014.979506.

[38] R. Rashid, N. S. J. Lim, S. M. L. Chee, S. N. Png, T. Wohland, and M. Raghunath, "Novel use for polyvinylpyrrolidone as a macromolecular crowder for enhanced extracellular matrix deposition and cell proliferation", *Tissue Engineering - Part C: Methods*, vol. 20, no. 12, pp. 994–1002, 2014, ISSN: 19373392. DOI: 10.1089/ten.tec.2013.0733.

[39] D. Shendi, J. Marzi, W. Linthicum, *et al.*, "Hyaluronic acid as a macromolecular crowding agent for production of cell-derived matrices", *Acta Biomaterialia*, vol. 100, pp. 292–305, 2019, ISSN: 18787568. DOI: 10.1016/j.actbio.2019.09.042. [Online]. Available: https://doi.org/10.1016/j.actbio.2019.09.042.

[40] S. Vasvani, P. Kulkarni, and D. Rawtani, "Hyaluronic acid: A review on its biology, aspects of drug delivery, route of administrations and a special emphasis on its approved marketed products and recent clinical studies", *International Journal of Biological Macromolecules*, vol. 151, pp. 1012–1029, 2020, ISSN: 18790003. DOI: 10.1016/j.ijbiomac.2019.11.066. [Online]. Available: https://doi.org/10.1016/j.ijbiomac.2019.11.066.

[41] K. M. Zia, S. Tabasum, M. Nasif, *et al.*, "A review on synthesis, properties and applications of natural polymer based carrageenan blends and composites", *International Journal of Biological Macromolecules*, vol. 96, pp. 282–301, 2017, ISSN: 18790003. DOI: 10.1016/j.ijbiomac.2016.11.095. [Online]. Available: http://dx.doi.org/10.1016/j.ijbiomac.2016.11.095.

[42] A. De Pieri, S. Rana, S. Korntner, and D. I. Zeugolis, "Seaweed polysaccharides as macromolecular crowding agents", *International Journal of Biological Macromolecules*, vol. 164, pp. 434–446, 2020, ISSN: 18790003. DOI: 10.1016/j.ijbiomac.2020.07.087. [Online]. Available: https://doi.org/10.1016/j.ijbiomac.2020.07.087.

[43] J. F. Burke, O. V. Yannas, W. C. Quinby, C. C. Bondoc, and W. K. Jung, "Successful use of a physiologically acceptable artificial skin in the treatment of extensive burn injury", *Annals of Surgery*, vol. 194, no. 4, pp. 413–427, 1981, ISSN: 00034932. DOI: 10.1097/00000658-198110000-00005.

[44] K. Vig, A. Chaudhari, S. Tripathi, *et al.*, "Advances in skin regeneration using tissue engineering", *International Journal of Molecular Sciences*, vol. 18, no. 4, 2017, ISSN: 14220067. DOI: 10.3390/ijms18040789.

[45] M. Varkey, J. Ding, and E. Tredget, "Advances in Skin Substitutes—Potential of Tissue Engineered Skin for Facilitating Anti-Fibrotic Healing", *Journal of Functional Biomaterials*, vol. 6, no. 3, pp. 547–563, 2015, ISSN: 2079-4983. DOI: 10.3390/jfb6030547.

[46] S. MacNeil, "Progress and opportunities for tissue-engineered skin", *Nature*, vol. 445, no. 7130, pp. 874–880, 2007, ISSN: 14764687. DOI: 10.1038/nature05664.

[47] G. B. Ralston, "Effects of 'crowding' in protein solutions", *Journal of Chemical Education*, vol. 67, no. 10, pp. 857–860, 1990, ISSN: 00219584. DOI: 10.1021/ed067p857.

[48] R. R. Lareu, K. H. Subramhanya, Y. Peng, *et al.*, "Collagen matrix deposition is dramatically enhanced in vitro when crowded with charged macromolecules: The biological relevance of the excluded volume effect", *FEBS Letters*, vol. 581, no. 14, pp. 2709–2714, 2007, ISSN: 00145793. DOI: 10.1016/j.febslet.2007.05.020.

[49] R. R. Lareu, I. Arsianti, H. K. Subramhanya, P. Yanxian, and M. Raghunath, "In vitro enhancement of collagen matrix formation and crosslinking for applications in tissue engineering: A preliminary study", *Tissue Engineering*, vol. 13, no. 2, pp. 385–391, 2007, ISSN: 10763279. DOI: 10.1089/ten.2006.0224.

[50] C. Z. Chen, Y. X. Peng, Z. B. Wang, *et al.*, "The Scar-in-a-Jar: Studying potential antifibrotic compounds from the epigenetic to extracellular level in a single well", *British Journal of Pharmacology*, vol. 158, no. 5, pp. 1196–1209, 2009, ISSN: 00071188. DOI: 10.1111/j.1476-5381.2009.00387.x.

[51] A. S. Zeiger, F. C. Loe, R. Li, M. Raghunath, and K. J. van Vliet, "Macromolecular crowding directs extracellular matrix organization and mesenchymal stem cell behavior", *PLoS ONE*, vol. 7, no. 5, 2012, ISSN: 19326203. DOI: 10.1371/journal.pone.0037904.

[52] P. Kumar, A. Satyam, X. Fan, *et al.*, "Macromolecularly crowded in vitro microenvironments accelerate the production of extracellular matrix-rich supramolecular assemblies", *Scientific Reports*, vol. 5, pp. 1–10, 2015, ISSN: 20452322. DOI: 10.1038/srep08729.

[53] S. Garnica-Galvez, S. H. Korntner, I. Skoufos, *et al.*, "Hyaluronic acid as macromolecular crowder in equine adipose-derived stem cell cultures", *Cells*, vol. 10, no. 4, pp. 1–20, 2021, ISSN: 20734409. DOI: 10.3390/cells10040859.

[54] A. Satyam, P. Kumar, X. Fan, *et al.*, "Macromolecular crowding meets tissue engineering by self-assembly: A paradigm shift in regenerative medicine", *Advanced Materials*, vol. 26, no. 19, pp. 3024–3034, 2014, ISSN: 15214095. DOI: 10.1002/adma.201304428.

[55] D. Gaspar, K. P. Fuller, and D. I. Zeugolis, "Polydispersity and negative charge are key modulators of extracellular matrix deposition under macromolecular crowding conditions", *Acta Biomaterialia*, vol. 88, pp. 197–210, 2019, ISSN: 18787568. DOI: 10.1016/j.actbio.2019.02.050. [Online]. Available: https://doi.org/10.1016/j.actbio.2019.02.050.

[56] A. Satyam, P. Kumar, D. Cigognini, A. Pandit, and D. I. Zeugolis, "Low, but not too low, oxygen tension and macromolecular crowding accelerate extracellular matrix deposition in human dermal fibroblast culture", *Acta Biomaterialia*, vol. 44, pp. 221–231, 2016, ISSN: 18787568. DOI: 10.1016/j.actbio.2016.08.008. [Online]. Available: http://dx.doi.org/10.1016/j.actbio.2016.08.008.

[57] D. Cigognini, D. Gaspar, P. Kumar, *et al.*, "Macromolecular crowding meets oxygen tension in human mesenchymal stem cell culture - A step closer to physiologically relevant in vitro organogenesis", *Scientific Reports*, vol. 6, no. April, pp. 1–11, 2016, ISSN: 20452322. DOI: 10.1038/srep30746. [Online]. Available: http://dx.doi.org/10.1038/srep30746.

[58] P. Kumar, A. Satyam, D. Cigognini, A. Pandit, and D. I. Zeugolis, "Low oxygen tension and macromolecular crowding accelerate extracellular matrix deposition in human corneal fibroblast culture", *Journal of Tissue Engineering and Regenerative Medicine*, vol. 12, no. 1, pp. 6–18, 2018, ISSN: 19327005. DOI: 10.1002/term.2283.

[59] D. Tsiapalis, S. Kearns, J. L. Kelly, and D. I. Zeugolis, "Growth factor and macromolecular crowding supplementation in human tenocyte culture", *Biomaterials and Biosystems*, vol. 1, no. January, p. 100 009, 2021, ISSN: 26665344. DOI: 10.1016/j.bbiosy.2021.100009. [Online]. Available: https://doi.org/10.1016/j.bbiosy.2021.100009.

[60] B. Chen, B. Wang, W. J. Zhang, G. Zhou, Y. Cao, and W. Liu, "Macromolecular crowding effect on cartilaginous matrix production: A comparison of two-dimensional and three-dimensional models", *Tissue Engineering - Part C: Methods*, vol. 19, no. 8, pp. 586–595, 2013, ISSN: 19373392. DOI: 10.1089/ten.tec.2012.0408.

[61] M. Cámara-Torres, R. Sinha, C. Mota, and L. Moroni, "Improving cell distribution on 3D additive manufactured scaffolds through engineered seeding media density and viscosity", *Acta Biomaterialia*, vol. 101, pp. 183–195, 2020, ISSN: 18787568. DOI: 10.1016/j.actbio.2019.11.020.

[62] D. Tsiapalis, S. Rana, M. Doulgkeroglou, *et al.*, *The effect of aligned electrospun fibers and macromolecular crowding in tenocyte culture*, 1st ed. Elsevier Inc., 2020, vol. 157, pp. 225–247, ISBN: 9780128201749. DOI: 10.1016/bs.mcb.2019.11.003. [Online]. Available: http://dx.doi.org/10.1016/bs.mcb.2019.11.003.

[63] C. W. Wong, C. F. LeGrand, B. F. Kinnear, *et al.*, "In Vitro Expansion of Keratinocytes on Human Dermal Fibroblast-Derived Matrix Retains Their Stem-Like Characteristics", *Scientific Reports*, vol. 9, no. 1, pp. 1–17, 2019, ISSN: 20452322. DOI: 10.1038/s41598-019-54793-9. [Online]. Available: http://dx.doi.org/10.1038/s41598-019-54793-9.

[64] A. Satyam, M. G. Tsokos, J. S. Tresback, D. I. Zeugolis, and G. C. Tsokos, "Cell-Derived Extracellular Matrix-Rich Biomimetic Substrate Supports Podocyte Proliferation, Differentiation, and Maintenance of Native Phenotype", *Advanced Functional Materials*, vol. 30, no. 44, pp. 1–11, 2020, ISSN: 16163028. DOI: 10.1002/adfm.201908752.

[65] S. Gomes, G. Rodrigues, G. Martins, C. Henriques, and J. C. Silva, "Evaluation of nanofibrous scaffolds obtained from blends of chitosan, gelatin and polycaprolactone for skin tissue engineering", *International Journal of Biological Macromolecules*, vol. 102, pp. 1174–1185, 2017, ISSN: 18790003. DOI: 10.1016/j.ijbiomac.2017.05.004. [Online]. Available: http://dx.doi.org/10.1016/j.ijbiomac.2017.05.004.

[66] J. K. Armstrong, R. B. Wenby, H. J. Meiselman, and T. C. Fisher, "The hydrodynamic radii of macromolecules and their effect on red blood cell aggregation", *Biophysical Journal*, vol. 87, no. 6, pp. 4259–4270, 2004, ISSN: 00063495. DOI: 10.1529/biophysj.104.047746. [Online]. Available: http://dx.doi.org/10.1529/biophysj.104.047746.

[67] C. Labno, "Two Ways to Count Cells with ImageJ", *Integrated Light Microscopy Core*, pp. 1–5, 2014. [Online]. Available: file:///C:/Users/ASUS/Desktop/Rujukan%20PhD/Clonogenic%20Assay/imagej%20colony%20counting%20protocol.pdf.

[68] Biotechne. "The importance of ihc/icc controls". (2022), [Online]. Available: https://www.rndsystems.com/resources/protocols/importance-ihcicc-controls (visited on 03/05/2022).

[69] C. G. Cole and J. J. Roberts, "The fluorescence of gelatin and its implications", *Imaging Science Journal*, vol. 45, no. 3-4, pp. 145–149, 1997, ISSN: 13682199. DOI: 10.1080/13682199.1997.11736396.

[70] Proteintech. "How to reduce autofluorescence". (2022), [Online]. Available: https://www.ptglab.com/news/blog/how-to-reduce-autofluorescence/ (visited on 03/05/2022).

[71] H. Hu, H. Hu, J. H. Xin, A. Chan, and L. He, "Glutaraldehyde-chitosan and poly (vinyl alcohol) blends, and fluorescence of their nano-silica composite films", *Carbohydrate Polymers*, vol. 91, no. 1, pp. 305–313, 2013, ISSN: 01448617. DOI: 10.1016/j.carbpol.2012.08.038. [Online]. Available: http://dx.doi.org/10.1016/j.carbpol.2012.08.038.

[72] B. Clancy and L. J. Cauller, "Reduction of background autofluorescence in brain sections following immersion in sodium borohydride", *Journal of Neuroscience Methods*, vol. 83, pp. 97–102, 1998. DOI: 10.1016/s0165-0270(98)00066-1.

[73] S. R. Gomes, G. Rodrigues, G. G. Martins, *et al.*, "In vitro and in vivo evaluation of electrospun nanofibers of PCL, chitosan and gelatin: A comparative study", *Materials Science and Engineering C*, vol. 46, pp. 348–358, 2015, ISSN: 09284931. DOI: 10.1016/j.msec.2014.10.051. [Online]. Available: http://dx.doi.org/10.1016/j.msec.2014.10.051.

[74] J. L. Ferreira, S. Gomes, C. Henriques, J. P. Borges, and J. C. Silva, "Electrospinning polycaprolactone dissolved in glacial acetic acid: Fiber production, nonwoven characterization, and in Vitro evaluation", *Journal of Applied Polymer Science*, vol. 131, no. 22, pp. 37–39, 2014, ISSN: 10974628. DOI: 10.1002/app.41068.

[75] X. M. Ang, M. H. Lee, A. Blocki, *et al.*, "Macromolecular crowding amplifies adipogenesis of human bone marrow-derived mesenchymal stem cells by enhancing the pro-adipogenic microenvironment", *Tissue Engineering - Part A*, vol. 20, no. 5-6, pp. 966–981, 2014, ISSN: 1937335X. DOI: 10.1089/ten.tea.2013.0337.

A

Literature Review Table

This appendix contains a table summarizing MMC-related work found in the literature.

Table A.1: Work in the literature utilizing MMC. Adapted from [28].

Crowders	Cells	Purpose	Results	Reference
100 μg/ml Dextran (Dx) 670 kDa; 100 μg/ml DxS 500 kDa	Human embryonic lung fibroblasts and adult hypertrophic scar fibroblasts	Effect of negatively charged macromolecules in the *in-vitro* procollagen processing	DxS 500 kDa outperformed Dx 670 kDa as it enhanced higher collagen deposition and induced higher lysyl oxidase activity	[49]
100 μg/ml DxS 10 kDa; 100 μg/ml DxS 500 kDa; 100 μg/ml PSS 200kDa; 50 mg/ml Fc 50 kDa & 50 mg/ml Fc 500 kDa	Embryonic lung fibroblasts	Effect of negatively charged macromolecules in ECM deposition	DxS 500 kDa and PSS 200 kDa induced a more accelerated conversion of procollagen type I to collagen type I, in comparison with neutrally charged macromolecules; Fibronectin deposition was not enhanced	[48]
100 μg/ml DxS 500 kDa; 37.5 mg/ml Fc 70 kDa & 25 mg/ml Fc 400 kDa cocktail	Human lung fibroblasts	Development of an *in vitro* model to study fibrosis	For faster collagen type I and fibronectin deposition (2 days), DxS should be used. For an increased deposition in 6 days, Fc cocktail should be used; MMC facilitated the development of a fibrotic *in vitro* model	[50]
37.5 mg/ml Fc 70 kDa & 25 mg/ml Fc 400 kDa cocktail	Human bone marrow MSCs	Effect in ECM deposition and organization and MSCs behavior	Increased deposition of collagen type I and type IV, and induced alignment of ECM fibers	[51]

37.5 mg/ml Fc 70 kDa & 25 mg/ml Fc 400 kDa cocktail	Porcine chondrocytes	Effect in 2D and 3D models	Increased collagen type II deposition and GAGs production in 2D models; In 3D models, MMC did not grant any advantage	[60]
100 μg/ml DxS 500 kDa; 37.5 mg/ml Fc 70 kDa & 25 mg/ml Fc 400 kDa cocktail; 75 μg/ml CR	Various cell types	Assessment of MMC in several cell types	Polydispersity and negative charge are important modulators of ECM deposition, with CR being associated to the highest ECM deposition	[54]
37.5 mg/ml Fc 70 kDa & 25 mg/ml Fc 400 kDa cocktail	Human bone marrow MSCs	Fasten of the protocol of adipogenic differentiation	Increase in the deposition of collagen type IV and fibronectin during adipogenesis; Decellularized deposited ECM fastened the adipogenic differentiation of MSCs	[75]
18.75 mg/ml Fc 70 kDa & 12.5 mg/ml Fc 400 kDa cocktail (9% v/v FVO); 21.5 mg/ml PVP 40 kDa (18% v/v FVO); 11.34 mg/ml PVP 360 kDa (54% v/v FVO)	Human dermal fibroblasts and human bone marrow MSCs	Assessment of ECM deposition	Fc mixture at 9% FVO induces greater collagen deposition than at 18% FVO; PVP 40 kDa induced the highest ECM deposition at 18% FVO; PVP 360 kDa induced the highest ECM deposition at 54%; Any PVP used did not outperform Fc mixtures at both 9% and 18% FVO	[38]
37.5 mg/ml Fc 70 kDa & 25 mg/ml Fc 400 kDa cocktail	Human corneal fibroblasts	Assessment of ECM deposition at low serum concentration	Increased the deposition of several collagenous proteins and fibronectin	[52]
37.5 mg/ml Fc 70 kDa & 25 mg/ml Fc 400 kDa cocktail	Human dermal fibroblasts and keratinocytes	Development of dermal-epidermal junction *in vitro*	Enhanced deposition of collagen type I and IV andfibronectin by fibroblasts; Increased deposition of collagen type VII by fibroblasts; Fibroblasts promote collagen production and deposition by keratinocytes	[31]
100 μg/ml CR at low oxygen tension	Human bone marrow MSCs	Assessment of multilineage potential of human marrow MSCs	Increased ECM deposition at both 2% and 20% oxygen tension	[57]

75 μg/ml CR	Human dermal fibroblasts	Assessment of ECM deposition at low serum concentration (0.5%), low oxygen tension (2%) and crowded conditions	Increased deposition of collagens type I, III, IV and V, and fibronectin	[56]
75 μg/ml CR	Human corneal fibroblasts	Assessment of ECM deposition under distinct oxygen tensions, serum concentrations and crowding conditions	Highest ECM deposition was achieved after 14 days in culture at 0.5% serum, 2% oxygen tension and 75 μg/ml CR	[58]
Several concentrations and molecular weights of CR, Fc (alone or in cocktail) and DxS (alone or in cocktail)	Human dermal fibroblasts	Assessment of ECM deposition	Negatively charged and polydispersed crowders induce the greatest ECM deposition; CR is the most effective crowder, however, mixtures of other crowders can induce significant ECM deposition as well	[55]
500 μg/ml HA 1500 kDa and 37.5 mg/ml Fc 70 kDa & 25 mg/ml Fc 400 kDa cocktail	Human dermal fibroblasts	Production of cell-derived matrices	HA did not significantly increase ECM gene expression or deposition	[39]
0.5, 1.5 and 10 mg/ml HA of different molecular weights (10, 60, 100, 500 and 1000 kDa)	Adipose-derived stem cells	Assessment of the influence of HA in adipose-derived stem cells	HA at different concentrations and molecular weights enhanced collagen type I, III and IV deposition, but did not outperform CR or Fc mixture	[53]
37.5 mg/ml Fc 70 kDa & 25 mg/ml Fc 400 kDa cocktail	Human dermal fibroblasts	Development of ECM-rich matrices for keratinocyte expansion	Enhanced deposition of collagen type I and IV; Decellularised matrix promoted keratinocyte proliferation	[63]
37.5 mg/ml Fc 70 kDa & 25 mg/ml Fc 400 kDa cocktail	Human dermal fibroblasts	Development of ECM-rich matrices for podocyte expansion	Increased deposition of collagens type I and IV and fibronectin; Decellularised matrix promoted podocyte proliferation and differentiation	[64]

50 μg/ml CR 550 kDa; 250 μg/ml ulvan 300 kDa; 50 μg/ml fucoidan 600 kDa; 50 μg/ml galactofucan 700 kDa	Human adipose-derived stem cells	Assessment of ECM deposition and effect on human adipose-derived stem cells differentiation	Fucoidan, galactofucan and ulvan enhanced collagen type I and collagen type V deposition, but were still outperformed by CR	[42]
50 μg/ml CR 550 kDa and growth factor supplementation (IGF-1, GDF5, TGFβ3, PDGF$\beta\beta$)	Human tenocytes	Effect of MMC and growth factors in tenocytes	CR with TGFβ3 induced the highest ECM deposition	[59]
50 μg/ml CR	Human tenocytes	Assessment of the combining effect of surface topography and MMC in human tenocytes	CR increased ECM deposition and promoted fiber alignment	[62]
Fc at 80, 60, 40 and 20 vol% in cell culture medium; Dx at 10, 5 and 2.5 wt% in cell culture medium	Human MSCs	Assessment of the influence of macromolecular crowders in cell seeding and distribution in 3D additive manufactured scaffolds	Cellular viability is maintained in the presence of the crowders; Improved cell distribution which led to increased ECM production	[61]

B

Protocols

This appendix contains various protocols used among the experimental work.

B.1 Matrix Preparation for Cell Culture

1. Immerse the matrices in v/v 70% ethanol during 20 minutes.
2. Remove the ethanol and wash 3 times with PBS.
3. After the removal of PBS, immerse the matrices in glycine, seal the recipient with parafilm and store it overnight at 4ºC. PCL matrices should not be immersed in glycine, being stored in PBS overnight.
4. In the following day, remove the liquid from the container and wash the matrices with PBS once.
5. After the removal of PBS, the matrices are ready to be used for culture.

B.2 Cell Culture

1. Aspirate culture medium from the T75 flask.
2. Wash the adhered cells with 10 mL of PBS, pouring the liquid in the corner and then gently shaking the flask to wash the whole surface.
3. Remove the solution and apply 1000 µl of TrypLE™ against the surface, gently swirling the liquid to cover all the cell monolayer.
4. Incubate during 5 minutes.
5. Remove from incubator and gently tap the sides of the flask in order to loosen the cells from the surface.
6. Add 10 mL of culture medium, resuspend several times and transfer the suspension to a falcon.

7. Proceed to cell counting, according to protocol B.2.1.

8. Transfer to a falcon the pretended quantity of cell suspension.

9. Centrifuge the suspension for 5 minutes at 200 relative centrifugal force (RCF), selecting the BRK5510 protocol.

10. Remove the liquid and add the pretended DMEM or MMC solution.

11. After mixing the added solution with the centrifuged cells, it is adequate to proceed to cell seeding.

B.2.1 Cell Counting

1. Add 20 µl of trypan blue stain (0.4%) and 20 µl of cell solution to an eppendorf and mix.

2. Prepare the hemocytometer by cleaning it with 70% ethanol and affix a coverslip onto it.

3. Fill both chambers underneath the coverslip with the suspension prepared in the eppendorf.

4. Using a microscope, focus on the grid lines of the hemocytometer with 10X objective.

5. Count the live cells, which appear brighter, inside each square limited from 3-line borders. Choose 3 squares, from a total of 9 squares (each chamber has 9 squares). To count the cells in the 3-line borders, only two out of four borders should be considered.

6. Move the hemocytometer to the other chamber, and repeat the process.

7. Cell density is calculated by equation B.1, where N is the total number of viable cells counted in all squares, 6 is the number of squares, 2 is the dilution factor and 10^4 is the chamber factor:

$$Cells/mL = \frac{N}{6} \times 2 \times 10^4 \tag{B.1}$$

8. Clean the hemocytometer and the coverslip with 70% ethanol and store at the proper glass container.

B.3 Resazurin Assay

1. Dilute the 0.4 mg/ml resazurin in PBS solution in low glucose DMEM supplemented with 1% Pen Strep and 10% FBS using a 1:1 (v/v) ratio.
2. Remove the culture medium from the wells and add 200 µl of the prepared solution.
3. Add 800 µl of the solution in an empty well, serving as the control group.
4. Incubate for 3 hours.
5. After incubation, transfer 140 µl of the solution from each well to a 96-well microplate.
6. Measure the microplate photometrically at 570 nm and 600 nm by the absorbance microplate reader (ELx800™, Biotek).

B.4 Immunofluorescence

For immunofluroescence, the following protocols were followed.

B.4.1 Fixing

1. Wash the wells 3 times with PBS++.
2. Apply 200 µl of fixing permeabilization solution for 5 minutes. Apply 200 µl of fixing solution for 20 minutes.
3. After removal of the previously applied solution, apply 200 µl of fixing solution for 20 minutes.
4. Remove fixing solution and wash 3 times with PBS.
5. Store at 4°C embedded in PBS or proceed to B.4.2.

B.4.2 Blocking

1. Apply v/v 0.5% Triton solution for 15 minutes.
2. After removing the solution, wash once with PBS.
3. Apply v/v 2% BSA in PBS for 1 hour at room temperature (RT).
4. Proceed to B.4.3

B.4.3 Staining

1. Apply fibronectin and collagen primary antibodies at 1:50 concentration in 2% BSA and leave overnight at 4ºC.
2. Wash thrice with PBS.
3. Exert fibronectin and collagen secondary antibodies at 1:50 and 1:100 concentration in 2% BSA, respectively, for 1h30 at RT. The samples should not be exposed to light.
4. Wash once with PBS.
5. Apply 4% DAPI in 2% PBS for 5 minutes.
6. Wash 4 times with PBS.
7. Wash twice with distilled water.
8. Utilize 10µl of Mowiol to mount the samples in glass surfaces.

B.4.4 Nuclei Counting

1. Open the intended image.
2. Go to 'Edit' →'Options' →'Conversions' and select the 'Weighted RGB Checked' option.
3. Go to 'Image' →'Type' and select '8-bit' option.
4. In tab 'Process', select the option 'Subtract Background'. Then, all the appearing options were not ticked, and the rolling ball radius selected was of 250 pixels.
5. Go to 'Image' →'Adjust' →'Threshold'. Then select the pretended 0-255 interval in order to maximize the number of nuclei and minimize the amount of noise.
6. Select 'Process' →'Binary' →'Fill Holes'.
7. Select 'Process' →'Binary' →'Watershed'.
8. Go to tab 'Analyze' and select 'Analyze Particles...'. Then, the ticked options were 'Display results', 'Clear results' and 'Summarize'. The selected size range was 500-Infinity, circularity range was 0.00-1.00 and outlines were shown.
9. The displayed results provide the number of nuclei counted in each image.

C

Statistics

Statistical tests are performed with the intent of assessing if there was enough evidence to reject the null hypothesis (H_0) about a certain data. The alternative hypothesis (H_1), which is the one the user would like to demonstrate, is compared to the null hypothesis and, if there is a statement of difference between both hypothesis, the null hypothesis should be rejected. However, the user should define a risk threshold, varying between a probability of 0 and 1, above which the null hypothesis should not be rejected, referred as the level of significance. If the obtained value from the test is inferior to that defined threshold, then the null hypothesis should be rejected with a probability of being wrong equal to the threshold. Several different types of statistic tests can be performed, but in this dissertation only Student's t-tests were performed.

C.1 Student's t-test

This statistical test compares the average value of two data-sets and analyzes if they are originated from the same population, with the null hypothesis assuming that both means are equal. The defined level of significance was 0.05. Microsoft Excel was used to perform t-tests using *T.TEST(array1,array2,tails,type)* function. Array1 and array2 are the data-sets to test, tails = 2 was used for a two-tailed distribution, and type = 3 to perform a two-sample unequal variance test. If the obtained result was inferior to 0.05 (p-value < 0.05), then the compared data-sets were significantly different (the null hypothesis is rejected with a confidence of 95%).